Modification of Brain Tumour Cell Migration via MEK Inhibitors

Romika Patel

A thesis submitted in partial fulfilment of the requirements for the degree of Masters in Biomedical Science, The University of Auckland, 2022.

Abstract

Glioblastoma (GBM) is an aggressive and heterogeneous primary brain tumour in adults. The current multimodal treatment includes surgical resection, chemotherapy, and radiotherapy. However, most patients experience recurrence, which is in part due to the highly migratory nature of GBM and the presence of glioblastoma stem-like cancer cells (GCSs) that exhibit stem-cell-like qualities and resistance against radiation and chemotherapy. Migratory molecules, such as polysialic acid neural cell adhesion molecule (PSA-NCAM), matrix metalloproteinases-9 (MMP-9) and phosphorylated focal adhesion kinase (pFAK), are considered to be involved in tumour cell migration. In addition, recent studies have highlighted associations between mitogen-activated protein/extracellular-signalling related kinase (MEK/ERK) cascade and GBM cell migration. This thesis aimed to investigate the effects of MEK inhibitors trametinib and U0126 on patient-derived GBM cells for the potential attenuation of tumour cell migration.

Both Trametinib and U0126 target the MEK-1 and MEK-2 subset and ultimately, inhibit downstream ERK phosphorylation and signalling. pERK and EdU assays were used to determine concentrations that effectively limited proliferation and had minimal toxicity. The concentrations were then administrated to tumour monolayered and spheroid cells in various experimentations including live cell, immunocytochemistry, western blot, qRT-PCR.

Overall, trametinib was more effective at inhibiting GBM tumour cell migration compared to U0126, and this finding was consistent across all experimental data. Some migratory markers displayed consistent changes when treated with trametinib, while others produced variable responses. However, no significant relationship was found between the chosen migratory markers and tumour cell migration in the presence of MEK inhibitors. Future prospects include repetition of experimentation in various patient-derived GBM cases and consideration of the tumour microenvironment and biology.

COVID-19 Impact Statement

The pandemic has heavily affected the experimentations undertaken in this thesis, as the year was filled with inconsistent lockdown periods. Initially, the research project involved the use of patient-derived glioblastoma cell lines to elucidate the effects of radiation on cell migration. This required extensive cell culture periods, followed by a length radiation selection process – all of which were severely affected by the February and August lockdowns.

The initial lockdown in 2021 resulted in the cessation of my cell cultures from the lack of maintenance and care. These patient-derived glioblastoma cell lines required a minimum of a month to re-establish and another month for the radiation selection process. During this time, my supervisor suggested slightly altering the scope of the research if another lockdown ensues. The research project now requires the use of patient-derived glioblastoma cell lines to investigate the use of MEK inhibitors in limiting tumour cell migration. This cell line also required extensive cell culture periods and was affected by the lockdown in August 2021.

The sudden lockdown in August affected my thesis the most as the newly cultured patient-derived glioblastoma cell lines had to be discarded again as no one was allowed to come into the lab during this period. Fortunately, I was allowed access to the lab near the end of the August lockdown. But, as we were in level 3 at that time, I could not access many of the key shared facilities which, further delayed any experimental progress that could have been undertaken during this period. The pandemic also heavily affected the delivery of key consumables such as cell media supplements and Matrigel, which were required for the maintenance and plating of cellular culture.

In summary, the majority of the experimentations stated in this thesis began around the end of November 2021 and were completed in late June 2022. Because of the COVID-19 disruptions, the scope of the research and the range of the experiments conducted were altered to fit into a shorter time frame. Despite the constant setbacks, I have learned several new techniques and analysis methods that have expanded my knowledge regarding brain tumours and tumour biology. I humbly request to consider the disruptions caused by COVID-19 when reviewing this thesis.

Thank you,
Romika Patel

Acknowledgements

Firstly, I would like to express my utmost gratitude to my supervisors, Dr. Thomas Park, Professor Michael Dragunow and Dr. Cho Rong Hong. Your support, guidance, patiences, and expertise were central in the completion of this research thesis amidst a global pandemic and the challenges that came along. Thank you Tom for taking me on board. I am grateful to have you as a supervisor who is stern yet understanding. Thank you for believing in me, even when things got tough. It has been an absolute honour and privilege to learn from you.

A massive and heartfelt thank you to the Park Team and Dragunow group. I appreciate all the support and guidance that was bestowed upon me. Grateful to have been a part of the CBR family. Special mention to the Night crew for being my comrades during all those late lab nights. Another special thanks to Richard at BIRU for helping me with complex cell analysis and imaging difficulties.

To my friends; Amandeep, Vicky, Matti, Hetal, Vattey, Harshikesh, and Nishalia – thank you for always supporting me and encouraging me during the tough times. I appreciate each and every one of you dearly.

Finally, thank you to my parents for all the support and love you have showered over me, especially during the final weeks of write up. Thank you to my sister Bhavini and brother-in law Rainesh for your unwavering belief in me and keeping me accountable. Thank you to Akshil for being my at-home supervisor and enduring my endless rambles about this project. I am very fortunate to have you in my life.

Last but not least, thank you to the donors and their families. Without their donations, this research would not have been possible.

Table of Contents

List of Figures

List of Tables

Chapter 1. General Introduction

Cancer is a devasting disease that nearly 10 million individuals worldwide succumbed to the disease in 2020 (Sung et al., 2021). It is identified by a population of uncontrolled and rapidly proliferating cells with dysfunctional cellular functions (Hanahan, 2022; Hanahan & Weinberg, 2011a). Brain tumours are cancer cells that either originate from brain tissue or nearby surrounding structures (*de novo/* primary brain tumours) or metastasise to the brain from other organs (secondary brain tumours) (Louis et al., 2016, 2021). The cellular origin of primary brain tumours can be further defined by two subsets, glial and non-glial tumours with glial tumours consisting of glial cells giving rise to anaplastic astrocytomas and glioblastomas for instance and non-glial tumours consisting of blood vessels, glands and nerves giving rise to meningioma (Lesniak & Brem, 2004). Within New Zealand, more than 300 people are diagnosed with brain cancer in 2016 (Yan et al., 2019).

The World Health Organisation (WHO) assembled a classification system that grades tumours based on the following parameters: the tumour severity, cellular behaviours and growth patterns exhibited by the tumour, presence of an isocitrate dehydrogenase mutation (IDH), histopathological necrosis and microvascular proliferation (Table 1) (Gupta & Dwivedi, 2017; Louis et al., 2021).

Table 1 World Health Organisation Classification of tumours based on the four morphologic features, including cytological atypia, mitotic activity, endothelial cell proliferation and necrosis. Tumours associated with each grade type are also displayed.

	Tumour Severity	Example
Grade I	▪ Slow growth ▪ Non-malignant and non-infiltrative ▪ Associated with long-term survival ▪ Possible to cure using surgery	o Craniopharyngioma o Gangliocytoma o Ganglioglioma
Grade II	▪ Tumour exhibits cytological atypia ▪ Slow growth but recurrent tumour can have a higher grade ▪ Can be malignant or non-malignant	o "Diffuse" Astrocytoma o Pineocytoma o Pure oligodendroglioma
Grade III	▪ Tumour exhibits anaplasia and mitotic activity ▪ Malignant and infiltrative ▪ Recurrent tumour can have a higher grade	o Anaplastic astrocytoma and ependymoma o Anaplastic oligodendroglioma
Grade IV	▪ Tumour exhibits anaplasia, mitotic activity with endothelial cell proliferation and/or necrosis ▪ Very aggressive and malignant ▪ Can infiltrate widely ▪ Rapid growth	o Glioblastoma (GBM) o Medulloblastoma o Ependymoblastoma

Roughly 80% of all primary malignant brain tumours fall under the umbrella of diffuse gliomas (Mulcahy et al., 2020). This subset of gliomas includes astrocytic tumours (or astrocytomas), oligodendrogliomas, oligoastrocytomas, glioblastomas, and ependymomas (Gupta & Dwivedi, 2017; Louis et al., 2007, 2016). Astrocytomas originate from star-shaped glial cells called astrocytes, which are abundant in the central nervous system in the normal brain where they support neuronal cells via synaptic mutation and provide nutrients (Mulcahy et al., 2020). An example of this tumour is glioblastoma (GBM). On the other hand, oligodendrogliomas originate from neural stem cells or glial progenitor cells, while ependymoma tumours arise from ependymal cells that line the ventricular system of the brain (Mulcahy et al., 2020). Most diffuse gliomas range between Grade I to III meaning they are the least malignant. But GBM, medulloblastoma and ependymoblastoma all belong to the grade IV category and have the greatest malignancy (Louis et al., 2007, 2016). The focus of my thesis will be on GBM, which will be further introduced in the following sections.

1.1. Introduction to Glioblastoma

Glioblastoma (GBM) is a heterogeneous and aggressive malignant primary brain tumour with a dismal prognosis (Louis et al., 2016; Smith et al., 2016; Taylor et al., 2019). This tumour is characterised by both intra- and inter-heterogeneity, making it a complex and challenging tumour to treat (Verhaak et al., 2010). The majority of GBMs are primary tumours that often develop rapidly in elderly patients, while secondary GBMs originate from lower grade diffuse or anaplastic astrocytomas and commonly diagnosed in young patients (Erasimus et al., 2016; Ohgaki & Kleihues, 2013). Primary and secondary GBMs are teased apart via genetic and epigenetic profiles such as Epidermal Growth Factor Receptor (EGFR) amplification and *TERT* promoter for primary GBM (Ohgaki & Kleihues, 2013). Previously, isocitrate dehydrogenase 1 (IDH) was used as a prognostic factor for GBM as well. However, in the 2021 WHO classification, IDH mutations were reclassified as a brand new subset of GBM tumours (Louis et al., 2021).

There is an extremely high chance of recurrence within patients due to the infiltrative nature of GBM, along with the presence of tumour-initiating glioma stem-like cells (GSCs) (Lee et al., 2006; Singh et al., 2003). These stem-like cells have been demonstrated to alter the effects of radiation and chemotherapy, leading to a reduction in sensitivity towards these treatments; hence, often associated with tumour recurrence (Lee et al., 2006) (discussed in depth later in the introduction).

This lethal tumour accounts for 329 individuals diagnosed with GBM in New Zealand (Patel et al., 2019b) and has a median survival of 15 months (Ghosh et al, 2017). Nearly all GBM cases are deemed sporadic and the most susceptible population is Caucasian males over 80 years old (Mulcahy et al., 2020; Ohgaki & Kleihues, 2013). Researchers have explored many speculated risk factors such as age, hormone changes, genetic susceptibility, and decreased immune response (Thakkar et al., 2014). A risk factor for GBM is the exposure to ionising radiation to the head and neck region, which increases the chance of GBM occurrence. This could be explained by the DNA damage induced by radiation and radiation-induced tumour cell migration (Butowski, 2015). Genetic syndrome such as Cowden, Turcot, Li-Fraumeni, Neurofibromatosis type 1 and type 2 are also associated risk factors of GBM, but only account for about 5% of GBM cases (Urbanska et al., 2014). Genetic alteration such as amplification of chromosome 7 and genomic deletions in chromosome 9p and 10q have been shown to have a poor prognosis (Crespo et al., 2011). The cancer genome atlas network have described molecular subtypes of GBM to be classical, mesenchymal, and proneural. These subtypes are based upon abnormalities in platelet-derived growth factor receptor-alpha (PDGFR-α), IDH, EGFR, and neurofibromin 1 genes (Verhaak et al., 2010). The classical and mesenchymal subtype is associated with unfavourable survival outcomes after chemotherapy and radiation (Chen & Xu, 2016). On the contrary, proneural subtype is linked with improved prognosis and survival rates, thought to be because of the mutations in the IDH gene (Q. Wang et al., 2017). As mentioned before, IDH mutation status was utilised as a prognostic factor for GBM and those with IDH mutations have a greater prognosis than those without the mutation (Brat & The Cancer Genome Atlas Research Network, 2015). But Ohgaki & Kleihues (2013) have concluded that IDH mutation is typically found in secondary GBM while wild-type IDH is found in primary GBM (Ohgaki & Kleihues, 2013).

1.2. GBM Treatment

1.2.1 **Stupp's protocol**

The current treatment regimen of GBM follows Stupp's protocol established in 2005, which aimed to increase overall patient survival and progression-free survival by combining surgery with radiation and temozolomide (TMZ) (Mulcahy et al., 2020; Stupp et al., 2005; Taylor et al., 2019; Yan et al., 2019). The treatment begins with maximal surgical resection to remove

greater volumes of tumour mass, which has been correlated greater overall survival (OS) and longer progression-free survival (PFS) (Mulcahy et al., 2020; Taylor et al., 2019; L. Wang et al., 2019). Though the surgery attempts remove the *majority* of the tumour, there are residual tumour cells that cannot be removed due to the complex nature and structure of the brain (Mulcahy et al., 2020). A balance is struck between gross total resection without inducing neurological defects and the quality of the patient's life (Orringer et al., 2012). To target these residual cells, adjuvant intervention is required in the form of radiation and chemotherapy to minimise the rate of residual tumour cell growth and migration, along with reducing the chance of recurrence.

In 1977, Professor Sheline concluded that radiation following surgery appeared to increase the survival rate for a maximum of roughly three years as most patients with grade IV lesions did not survive up to the fifth year mark. He hypothesised that adding chemotherapy after radiation treatment may improve patient survival (Sheline, 1977). Many years later, Stupp et al. (2005) discovered Sheline's hypothesis of combining radiation- and chemotherapy (TMZ) to be true as it led to an increase in patient survival compared to radiation therapy alone. Specifically, an increase in the OS from 12.1 months (radiation alone) to 14.6 months (combination of radiation and chemotherapy) (Stupp et al., 2005) provided hope to many fighting this cruel disease.

In greater detail, Stupp's protocol consists of radiation therapy that targets the residual tumour cells via beam of ionising radiation (Sheline, 1977; Sulman et al., 2017), along with chemotherapy with temozolomide. Briefly, temozolomide is an oral DNA alkylating agents and attaches methyl group to the purine bases of DNA (that is adenosine and guanine) (Stupp et al., 2005; Zhang et al., 2012). The treatment regime typically comprises a total of 60 gy radiation administrated as 2 gy fractionated doses over the course of a few months with 150-200 mg/m^2/ day of temozolomide for 5 days every 28 days duration (Stupp et al., 2005). This is followed by another 6 months of temozolomide prescribed 5 days a month.

1.2.2 **Radiation**

Radiation therapy is critical in the management of cancers, whether it be brain tumours, prostate, breast or skin cancers (Baskar et al., 2012; Gianfaldoni et al., 2017). Nearly 50% of all cancer patients receive this therapy either before or after surgery (Begg et al., 2011). Ionizing radiation targets residual tumour cells following surgery (adjuvant) or tumours located in "hard to reach" places via deposition of electrically charged particles into cells.

This deposition limits the ability of tumour cells to undergo cell division and proliferation as their DNA is damaged by the ionizing radiation (S. P. Jackson & Bartek, 2009). Normal cells are able to repair themselves more efficiently than tumour cells after radiation therapy, leading to preferential elimination (Begg et al., 2011). The fractionation regimen of radiation therapy is based on normal cells proliferating slowly, and so these are able to repair any DNA damage sustained from radiation while rapidly proliferating tumour cells are targeted (Ellis, 1969). Therefore, radiation therapy aims to maximise the exposure of radiation to residual tumour cells, while reducing exposure to healthy surrounding cells (Baskar et al., 2012; Sheline, 1977; Sulman et al., 2017).

Radiation therapy works via direct and indirect damage, where the former *directly* interacts with DNA to induce damage, while the latter produces free radicals to induce damage. Both methods converge at the point of cellular death, where irreparable double-stranded breaks are formed in the DNA, leading to the slow downfall of tumour cells (Baskar et al., 2012). In the case of GBM, external radiation therapy (Intensity-modulated radiation therapy) is provided to patients as precise manipulation of photons and proton beams of radiation is utilised to match the shape of the tumour (Baskar et al., 2012). This precision minimises the damage to healthy surrounding tissue. Multiple exposures of radiation are required for radiation therapy to be deemed effective, hence the fractionation regimen. Many radiologists typically prescribe fractionated doses between 1-3 gy over a couple of weeks (Baskar et al., 2012) since it was found to be the most optimal, accumulating to a total of 60 gy doses. Overall, radiation therapy decreases tumour cell proliferation and increases the overall survival by 6-8 months (Sulman et al., 2017).

In recent years, researchers have discovered tumour cells are becoming radiation resistant. This adds to another layer of complexity to be considered when developing therapeutic treatments. As radiation is given to target residual cells, it is possible that these cells develop radiation resistance and migrate into the surrounding healthy tissue (Carruthers et al., 2015; Wild-Bode et al., 2001). This phenomenon occurs in GBM tumours and is considered to be due to glioblastoma stem-like cancer cells (GSCs) (M. Jackson et al., 2014) (expanded upon later on).

1.2.3 **Chemotherapy via TMZ**

Temozolomide (TMZ) is an oral alkylating agent that targets the levels of DNA-repairing enzyme, O^6-methylguanine-DNA methyltransferase (MGMT) in tumours by producing

highly reactive methyldiazonium cations. These cations methylate the DNA bases, specifically the O^6 guanine position and cause DNA damage, leading to cell cycle arrest (J. Zhang et al., 2012).

The effects of TMZ are reversed when MGMT promoter is unmethylated as the activated enzyme remove the alkylation of guanine and causes DNA replication to resume as normal. But, when the promoter is methylated, TMZ produces DNA damage and leads to longer patient survival (Stupp et al., 2005) since the tumour is unable to replicate infinitely. This causes a cycle of futile DNA repair and sends the tumour down the senescence or apoptotic pathway (L. Liu & Gerson2, 1996; Ochs & Kaina, 2000). MGMT methylation status serves as a prognostic factor in tumours, with nearly 50% of all patients displaying MGMT promoter being methylated and within those patients, TMZ is effective (Hegi et al., 2005). This is due to the epigenetic silencing of the MGMT gene via TMZ-induced promoter methylation and diminishes DNA-repair activity, as well as loss of MGMT expression (Qian & Brent, 1997).

While exploring the addition of TMZ to a short-course radiation treatment, (Perry et al. (2017) observed longer overall survival of the elderly GBM patients during the six-week period, compared to radiotherapy alone (Perry et al., 2017). This suggests that a combination of radiation and chemotherapy is beneficial in tackling this multifaceted cancer.

1.2.4 **Pharmacological Intervention via MEK Inhibitors**

Mitogen-activated protein kinase kinase (MEK) inhibitors have been widely used in the treatment of various cancers as the mitogen-activated protein kinase (MAPK) signalling cascade relays many cellular signals and interacts with other cellular pathways (Chappell et al., 2011; Sunayama et al., 2010). This thesis will focus on trametinib and U0126 which are both inhibitors of MEK (the MEK/extracellular signal-regulated kinase (ERK) signalling pathway is expanded in subsection 1.4).

Trametinib is an FDA-approved oral MEK inhibitor initially produced for the treatment of *BRAF*^{V600} mutant metastatic melanoma (Thota et al., 2015). In a phase III clinical trial, trametinib significantly improved response rates and median progression-free survival (PFS) compared with chemotherapy (Flaherty et al., 2012). These responses are most likely due to the pharmacokinetics of trametinib as the drug is a highly potent reversible allosteric inhibitor

of MEK-1 and MEK-2 (Thota et al., 2015). Since then, the effects of this drug have been investigated in various other cancers, including GBM.

U0126 is a non-competitive MEK-1 and MEK-2 inhibitor but has failed to be considered an effective inhibitor (Duncia et al., 1998). The drug also attenuates MEK5 and ERK5 signalling (Davies et al., 2000). U0126 is commonly used in many MEK/ERK signalling studies to attenuate the pathway, but the drug serves as a comparison molecule rather than being the hero.

1.3. Cellular Migration

1.3.1 **Normal Migration**

Cellular migration serves a crucial function in wound repair, embryonic development, and immune response (Friedl & Gilmour, 2009; Fu et al., 2019; Kurosaka & Kashina, 2008; Ve Chazal et al., 2000). By birth, neurogenesis, which is the generation of neurons from neural stem cells, is nearly complete (Cayre et al., 2009; Murray et al., 2016). While, in the adult brain, neural cell migration is minimal and limited to the subventricular zone and the dentate gyrus of the hippocampus (Cayre et al., 2009). Often during the development of brain tumours, cellular migration methods are hijacked and contribute to the development and metastatic of tumour cells (Hanahan & Weinberg, 2011a).

1.3.2 **Migration in Various Cancers/ in Cancer Cells**

Directed migration of tumours into surrounding tissues is considered one of the hallmarks of cancer (Gerashchenko et al., 2019; Hanahan & Weinberg, 2011b). This invasion is possible via various phenotypic transitions, including epithelial-mesenchymal, and contributes to the diversity in migration patterns and mechanisms (Gerashchenko et al., 2019).

The first step of tumour metastasis begins with the detachment of malignant cells from the tumour bulk, which gain active migratory abilities and invades adjacent tissues (Sahai, 2005). Typically, cancer cells from the invasive front, which is the interface between the tumour and healthy cells, initiate migration as it is believed that these cells have acquired locomotor phenotype (Bànkfalvi et al., 2000; Zlobec & Lugli, 2009) and result in either collective or individual tumour migration (Sahai, 2005).

Briefly, collective cell migration utilises adhesion molecules, the presence of leader cells which express basal epithelial genetic program, rich in cytokeratin-14 and transcription factor p63 (Cheung & Ewald, 2014) and form lamellipodia resulting in pulling following cells and disruption of the extracellular matrix via proteases (Pandya et al., 2017; X. Wang et al., 2016).

On the other hand, individual cells migrate via mesenchymal and amoeboid mechanisms (Paňková et al., 2010). In the former, tumour cells exhibit a fibroblast-like phenotype, high integrin expression, proteolytic enzyme production, lamellipodia and actomyosin contractions (Pandya et al., 2017). In the latter, tumour cells exhibiting actomyosin machinery and protrusion formation depend on Rho/ROCK signalling and type II myosin activity (Paňková et al., 2010).

Epithelial-mesenchymal transition (EMT) is when tumour cells shed epithelial characteristics and adopt mesenchymal features, along with resistance to therapeutics and prevention of apoptosis (Lamouille et al., 2014). It is an important process for tumour migration, invasion, and metastasis, along with regulating apoptosis and stemness of cells (Savagner, 2015). EMT is activated via molecular changes in tumour cells and the presence of cytokines and growth factors produced by immune and stromal cells within the tumour microenvironment (D. Gao et al., 2012; Lambert et al., 2017). Partial EMT (where cells retain epithelial features but have obtained mesenchymal traits) is more commonly observed in tumour budding cells (a group of cells) that are found in the invasive front and are associated with elevated metastasis and dismal prognosis in many cancers (Grigore et al., 2016). Activation of EMT transcription factors (snail, twist, and zeb) is enough to trigger single-cell dissemination without activating the whole EMT, and so the tumour cell retains its epithelial identity (Cheung & Ewald, 2014).

The basement membrane (comprising of laminins, type IV collagen) and other components (Rowe & Weiss, 2009) are impaired during tumour migration (Pandya et al., 2017). The interaction among laminin-5 and tumour integrins produces proteases and degrade the basement membrane and extracellular matrix (ECM) (Sharma et al., 2013). Following this, tumour cells invade the ECM and stimulate the once physically protective fibronectin to activate ECM proteolysis via metalloproteinases, MMP-2 and MMP-9 (Rowe & Weiss, 2009). In various cancers, fibronectin is a regulator of tumour migration and invasion (J. P. Wang & Hielscher, 2017).

1.4. MAPK/ERK Signalling

When activated, the MAPK/ERK signalling pathway produces downstream transcriptional changes to induce proliferation, differentiation, and migration (Dhillon et al., 2007; Guo et al., 2020). Briefly, the tyrosine kinase receptors located at the cell surface are stimulated through various growth factors, including PDGF, FGF, and EGF. This results in the activation of the phosphorylation cascade via the RAS/Raf/MEK/ERK proteins (Guo et al., 2020). MEK is a serine/threonine kinase and tyrosine kinase causing the protein to have a dual function. It is located upstream of ERK and regulates many transcription factors including Ets-1, cMyc and c-Jun (Alessi et al., 1994; Chappell et al., 2011). ERK is involved in the activation of other transcription factors such as CREB and NFκB, which stimulate genes associated with proliferation and survival (Chang et al., 2003; Steelman et al., 2004).

MEK/ERK signalling pathway is commonly upregulated in GBM pathogenesis and has been theorised to partake in the possibly limitless replication by the tumour. Alterations in this pathway lead to tumour cell cycle checkpoint evasion, nullify apoptosis, the overexpression of growth factors and cell surface receptors, which ultimately leads to tumour cell migration, proliferation and metastasis (McLendon et al., 2008).

Through the use of berberine, an isoquinoline alkaloid present in many herbal medications, an attenuation of the MEK/ERK pathway was seen with the stimulation of senescence in GBM (Q. Liu et al., 2015). In addition, treatment of A172 glioblastoma with PI3K and MEK inhibitors in results in a reduction of downstream gene effectors Bmi1, SOX2, and nestin, Furthermore, a reduction in tumoursphere was elicited by both drugs and caused a modulation in the replication potential of GBM as the pro-differentiation effect was also observed in these cells (Sunayama et al., 2010).

This pathway has the ability to activate various downstream effectors involved in tumour cell migration, proliferation, and metastasis and other signalling pathways making MAPK/ERK signalling pathway an attractive target for therapeutic intervention. Targeting the MAPK signalling cascade becomes further complicated due to intra-tumoural heterogeneity, co-amplification, and alteration in tyrosine kinases (McLendon et al., 2008).

1.5. Current Gaps In Our Knowledge

1.5.1 **Problem at hand**

Surgery is not curative (M. Jackson et al., 2014) as there are often residual tumour cells present post-surgery due to the invasive nature of high-grade brain tumours. Radiation is administered to eliminate or at most reduce these residual cells (Sheline, 1977; Sulman et al., 2017), and in some cases, this is sufficient. However, in the majority of the cases, recurrence emerges as residual cells "slip away" into healthy surrounding brain tissue (Carruthers et al., 2015; M. Jackson et al., 2014; Shankar et al., 2014; Smith et al., 2016). Many have speculated that recurrence is caused by treatment-resistant tumour-initiating stem-like cells (GSCs) (Bao et al., 2006; Sanai et al., 2005; Silvestri et al., 2014) that ultimately repopulate the tumour and further tumour migration

1.5.2 **Stem-like GBM cells**

Tumour recurrence has been attributed to a subpopulation of GBM cells termed Glioblastoma stem-like cancer cells (GSCs) that display a stem cell-like profile and are resistant to both radiation and chemotherapy (Bao et al., 2006; Sanai et al., 2005; Zepecki et al., 2019). These stem-like cells possess the ability to differentiation into various cell types, including neuronal and astrocytic cells (Lan et al., 2017). Zepecki et al., (2019) and others have demonstrated an embryonic stem cell-like signature in GBM and inhibition of this signature results in reduced GBM growth and GSCs (Zepecki et al., 2019). This embryonic stem cell-like signature comprised of core stem cell regulators that mediate pluripotency and stemness, including NANOG, OCT4, and SOX2, which control stem cell expansion and self-renewal (Zbinden et al., 2010). Along with the core stem cell regulators, GSCs also express Sonic Hedgehog (SHH), GL1, Notch-1, Wnt/beta-catenin and they are associated with sustaining long-term self-renewal and propagation, making GSCs similar to normal neural stem cells (Silvestri et al., 2014).

The cell cycling rate for GSCs is slower than the bulk of tumour consisting of rapidly proliferating tumour cells (Tang et al., 2019). Current therapeutics are designed to target the rapidly proliferating tumour cells, yet disregard the slow proliferating GSCs. This enables GSCs remaining in the tumour origin to possibly resume proliferation, invasion, and

experience changes in tumour biology for the development of resistance against treatments, for instance, chemotherapy and radiation (Pollard et al., 2009).

In summation, it is widely speculated that these GSCs are responsible for recurrence and treatment resistance and, it is imperative to understand the possible mechanisms these cells are undertaking to contribute to resistance and recurrence.

1.5.3 **Tumour Cell Migration Models**

Tumour cell migration is generally investigated through the use of *in vitro* migration assay techniques, including wound healing, transwell migration, and mechanical scratching. Briefly, the wound healing assay is conducted by creating a cell-free region at the bottom of the well by mechanical scratching (Riahi et al., 2012)

Similar to the wound healing assay, the mechanical scratching assay is also conducted by scratching a cell-free region at the bottom of the well, but this assay requires multiple scratches in the monolayered cells (Btirk, 1973; Yue et al., 2010). On the other hand, the transwell migration assay (also known as the Boyden chamber assay) uses a porous membrane where cells migrate through the porous membrane due to the differences in serum media concentration gradient (Kramer et al., 2013). These techniques used two-dimensional monolayer cell cultures where tumour cells adhere to the base of the well and appear in a singular layer (Duval et al., 2017; Kramer et al., 2013).

These current models fail to accurately represent tumour cell migration that occurs within patients as the tumour cells form a monolayer on the base of the well, which restricts cellular movement to a single plane and the morphology adopted by GBM tumour cells consist of a three dimensional sphere. Thus, the use of spheroid assays is becoming popular over the years as it fuses two-dimensional and three-dimensional technologies for a better representation of cell-cell contacts, tissue-like morphology and the tumour microenvironment (Duval et al., 2017; Kramer et al., 2013). The spheroid assay has been utilised in various GBM migration studies. For instance, the study conducted by Deryugina and Bourdon demonstrated the use of spheroid assay to examine glioma tumoursphere cell migration (Deryugina & Bourdon, 1996). But, many in the field still use more conventional assays to explore GBM migration (Younis et al., 2019; Yue et al., 2010) as they are simple, cost-effective, and high-throughput.

Though, improvements in the tumour cell migration model are required for future cell migration assays to reflect the tumour present within most patients, as many fail to consider all aspects of tumour biology and microenvironment.

1.6. Potential Migratory Molecules Mediating Tumour Cell Migration

Cellular proliferation and migration are involved at every stage of brain development, from embryonic to adult brain development (Cayre et al., 2009). Under normal physiological conditions, cellular migration is involved in building new synaptic connections, neuronal migration, and refinement of the neuronal circuit (Cayre et al., 2009). On the other hand, tumour cells, such as GBM, can utilise these mechanisms to escape radiation treatment (Biserova et al., 2021; Sahai, 2005). Furthermore, tumour development processes, including tissue invasion and migration heavily dependent on the change in the expression or function of cell adhesion molecules to become malignant (Hanahan & Weinberg, 2011a; Seifert et al., 2012). These altered cell adhesion molecules are referred to as migratory markers throughout this thesis. The following migratory markers are believed to be involved in the migration and invasion of cells in GBM: neural cell adhesion (NCAM), polysialylated neural cell adhesion molecule (PSA-NCAM), ST8Sia II (STX), ST8Sia IV (PST), L1 protein cell adhesion molecule (L1CAM) and SRC-family kinases (pFAK).

1.6.1 **Neural cell adhesion molecule (NCAM)**

NCAM belongs to the immunoglobulin (Ig) superfamily and partakes in many neurological processes during and following development, such as neuronal plasticity and neurogenesis (Mione et al., 2016). The molecule interacts with various ECM components such as heparin, collagen, chondroitinsulfate and is a crucial mediator of cell-cell and cell-substrate binding (Al-Saraireh et al., 2013; Fujimoto et al., 2001). NCAM is highly concentrated at the cell-cell contact sites for cell adhesion (Seidenfaden et al., 2003). Within the rostral migratory stream (RMS), NCAM aids in the uniform cellular organisation of neuronal precursor cells (Seidenfaden et al., 2003). Deficiency in NCAM produces a thicker RMS as migrating neuronal precursor cells accumulate in the stream and ultimately causes a reduction in the olfactory bulb (Cremer et al., 1994; Tomasiewicz et al., 1993).

High structural diversity is present in NCAM due to dynamically mediated post-translational modification, and alternative splicing (Crossin & Krushel, 2000), leading to different isoforms of NCAM existing as a consequence. The presence of a transmembrane domain

defines the NCAM-140 isoform, while a lack of the domain defines NCAM-120 (Suzuki et al., 2005). NCAM expresses homophilic, heterophilic, and trans-binding with other cell adhesion molecules, including L1CAM, protease-resistant protein and TAG-1 (Hoffman & Edelman, 1983; Horstkorte et al., 1993; Seifert et al., 2012).

The most notable transformation of NCAM is the attachment of polysialic acid (polySia) onto one of the six possible N-linked glycosylation sites, which carries the negatively charged polysia and results in the polysialylated neural cell adhesion molecule, PSA-NCAM (Seifert et al., 2012) (discussed further in the following subsection). Some studies have revealed that the degree of NCAM sialylation mediates its ability to stimulate cell adhesion (Cremer et al., 2000; Mione et al., 2016).

In some tumours, the expression of NCAM (without polySia) has reduced the aggressive nature of the tumour and inversely correlates with metastatic dissemination. For instance, NCAM expression reduces progression towards malignant glioma (Sasaki et al., 1998), and an increased NCAM expression in multiple myeloma cells is associated with decreased bone marrow infiltration (Sahara & Takeshita, 2004). This is due to the cell adhesion function of the molecule (Seifert et al., 2012).

1.6.2 **Polysialylated neural cell adhesion molecule (PSA-NCAM)**

Polysialic acid is a carbohydrate that can be attached to NCAM via post-translational modification (Cremer et al., 2000). This modification diminishes cell-cell adhesion and cell-other surface interaction of NCAMs (Fujimoto et al., 2001). In addition, polysialic acid (PSA) prevents premature neural differentiation (Petridis et al., 2004; Seidenfaden et al., 2003).

Polysialic transferase enzymes sialyltransferase-X (STX/ST8SiaII) and polysialyltransferase (PST/ST8SiaIV) synthase attach sialic acids onto the Ig-like domain of NCAM within the golgi, which is then expressed on the surface of NCAM (Kojima et al., 1996; Muhlenhoff et al., 1996). These two enzymes will be discussed in greater detail later on.

The post-translational modification reduces the interactions between NCAM and the extracellular matrix (ECM), enabling the cell to be “slippery” and migrate (Cayre et al., 2009; Fujimoto et al., 2001; Guan et al., 2015; Johnson et al., 2005). This molecule is important in

cellular migration (Cremer et al., 2000), neural development (Ditlevsen et al., 2008), neurogenesis (Rutishauser, 2008), and synaptic plasticity (Muller et al., 1996) in both developing and adult brains.

During normal brain development and adult neurogenesis, PSA-NCAM regulates chain neuroblast migration in the rostral migratory stream (Seifert et al., 2012). In 2007, PSA-NCAM on neuronal precursor cells migrating from the subventricular zone through the rostral migratory stream to the olfactory bulk was discovered in adult human brains (Curtis et al., 2007). PSA-NCAM is limited to specific areas that undergo structural and functional plasticity in adult brains (Seki & Arai, 1993; Theodosis et al., 1991). Studies have shown that PSA-NCAM positive cells regulate cell migration in the dentate gyrus and subventricular zones (Hu & Tomasiewicz, 1996; Ve Chazal et al., 2000). The absence of PSA-NCAM causes ineffective migration of cells due to improper formation of neuronal progenitor chains, causing cells to accumulate in the subventricular zone (Hu & Tomasiewicz, 1996).

Some studies have explored inhibiting PSA-NCAM via enzymatic methods, such as endoneuraminidase-N (endo-N), or genetic methods, including NCAM knock-out mice, to establish the function of PSA-NCAM in a normal adult brain. The enzymatic removal of PSA-NCAM via endoN increases in the interactions between NCAM and ECM, leading to decreased migration and aberrant differentiation of dispersed neuroblasts (Battista & Rutishauser, 2010; Ve Chazal et al., 2000). In addition, authors Gundelach and Koch discovered that treatment with endo-N caused widening of RMS and disruptions to the generally uniform cellular orientation of RMS. This lead to neuroblast cells leaving the RMS and migrating toward the lesioned tissue in rats (Gundelach & Koch, 2020). Furthermore, removal via endo-N resulted in premature differentiation in the SVZ-progenitor cells. Therefore, enzymatic removal of PSA-NCAM significantly decreased the migration abilities of neuroblastoma cells (Petridis et al., 2004), a phenomenon that may be utilised to reduce migration of the stem-like GBM cells.

In recent years, several studies have highlighted a possible contribution by PSA-NCAM in the stimulation of tumour migration and prevention of differentiation (M.-C. Amoureux et al., 2010; Suzuki et al., 2005). A study by Suzuki et al., (2005) discovered levels of PSA-NCAM expression directly correlated with tumour invasiveness when they transplanted STX and PST in C6 glioma cell lines into mice brains. C6 cells that were positive for PSA-NCAM migrated further into the corpus callosum compared to the PSA-NCAM negative cells

(Suzuki et al., 2005). In support, a study by Amoureux et al., (2010) displayed reduced overall survival and disease-free survival in patients with PSA-NCAM protein levels greater than 10pg/ug, which was associated with human glial tumours and its invasiveness. The authors of the study suggested that PSA-NCAM is an adverse prognostic factor in GBM (M.-C. Amoureux et al., 2010). In addition, Seidenfaden et al., (2003) found that when polysialic acid is downregulated (that is downregulation of PSA-NCAM), tumour cells cease proliferation and begin to differentiate (Seidenfaden et al., 2003). In our experiments, we have also seen the level of PSA-NCAM expression in patient tumours negatively correlate with patient survival (unpublished data). This finding partly forms the basis of this thesis.

In summary, researchers have concluded polysialylation of NCAM serves as a switch between tumour-suppression and tumour-promotion as the NCAM molecule (without polySia) has cell adhesion functions, while the addition of polySia causes sterical hinderance of NCAM-NCAM and other NCAM interactions (Johnson et al., 2005). Therefore, there is sufficient evidence that PSA-NCAM heavily contributes to tumour migration and invasion in GBM and other brain tumours.

1.6.3 **ST8Sia II (STX) & ST8Sia IV (PST)**

As mentioned prior, STX (ST8SiaII) and PST (ST8SiaIV) are two golgi-associated enzymes that attach the polysialic acid units to NCAM (Kojima et al., 1996; Muhlenhoff et al., 1996; Seifert et al., 2012). There is a direct correlation between the polysialylation of NCAM and the expression of STX and PST (Hildebrandt et al., 1998). During development, STX expression is the most dominant and gradually reduces after birth. On the other hand, PST expression is dominant in the adult brain (Mione et al., 2016). These two enzymes were explored in this thesis as they are involved in the post-translational modification of NCAM and regulators of PSA-NCAM.

Mione et al., (2006) explored the expression of both enzymes in the olfactory bulbs of adult rats and concluded a distinct expression pattern where immature rodent cells expressed STX while mature cells expressed PST (Mione et al., 2016). However, some researchers strongly speculate that altered expression of STX is involved in polysialylation of NCAM in tumours and contributes to tumour migration and invasion. For instance, in non-small lung cell carcinoma, the PST gene had equal expression between normal and tumour lung tissue. On

the other hand, the STX gene produced a greater expression in tumour lung tissue compared to normal tissue (Tanaka & Kawano, 2000). Author Seifert proposes it is possible to reduce polysialylation of NCAM and switch back to tumour-suppression functions of NCAM by targeting the STX enzyme (Seifert et al., 2012).

1.6.4 **Other markers of interest that may supplement migratory markers**

Other migratory markers that are of interest that will be explored in this study include Ki67, pFAK, and MMP-9.

Ki67 is a well-defined cell proliferation marker and is considered to facilitate tumour development dissemination, migration, and growth (X. Sun & Kaufman, 2018). In breast cancer, nuclear expression of Ki67 is two-fold greater at the invasive front compared to other regions of the tumour (Gong et al., 2013).

Metalloproteinases such as MMP-9 are involved with cytoplasmic rearrangement in the cells via proteolytic degradation of the basement membrane and extracellular matrix (ECM). For instance, MMP-9 directly degrades the ECM (Lakka et al., 2002), and elevated expression of MMP-9 at the invasive front of various cancers has been noted (Planagumà et al., 2011). Some studies have shown that MMP-9 is associated with MEK/ERK signalling as altered phosphorylation of ERK1/2 results in down-regulation of MMP-9 (Dontula et al., 2013)

Through the interactions with focal adhesion kinase (FAK), the SRC-family kinases (SFKs) are able to mediate intracellular signalling pathways (Ditlevsen et al., 2008). By phosphorylating FAK (attachment of phosphorus group to FAK molecule), SFKs regulate cytoskeleton organisation and remodelling associated with cell migration, adhesion, and division in response to ECM (Ahluwalia et al., 2010). Ultimately SFKs can disrupt cell-cell adhesion and promote invasion in tumours (Ditlevsen et al., 2008). Some have suggested that inhibiting SRC/FAK may aid in limiting tumour growth and migration (Ahluwalia et al., 2010), and this may be effective in GBM patients since the tumour is considered highly invasive.

1.7. Thesis outline/aims

The current multimodal treatment of GBM includes surgical resection, chemotherapy, and radiotherapy, but is considered inadequate. This is because many patients experience GBM recurrence, which is speculated to be due to the highly migratory nature of GBM. Recent studies have highlighted potential links between GBM migration and the MAPK signalling cascade, notably MEK/ERK signalling contributing to GBM tumour migration and invasion. Moreover, the presence of glioblastoma stem-like cancer cells (GCSs) is also speculated to contribute to GBM recurrence. This thesis aims to investigate the effects of MEK inhibitors trametinib and U0126 on the potential limitation of GBM tumour cell migration. Furthermore, the thesis aims to explore any differences between monolayered tumour cells and spheroid tumour cells concerning migratory markers.

Chapter 2. General Methods

2.1. Tissue Sources

The primary GBM cell sample used in this thesis was obtained with consent from patient donors undergoing therapeutic surgical resection performed at Auckland City Hospital. Ethical approval by the University of Auckland Human Participants Ethics and the Northern Regional Ethics Committee was obtained before any experimentation began. Table 2 summarises all the biopsy information for the GBM cases used in this thesis.

Table 2 Characteristics of all GBM tissue samples used for experimentation

Case Number	Age	Sex	Pathology	WHO Classification (grade)*	MGMT Status
T115	67	Male	GBM	IV	Unmethylated
T84	69	Male	GBM	IV	Undefined
T146	60	Male	GBM	IV	Methylated

*The WHO classification is explained in greater detail (see table 1 in chapter 1)

Note: The majority of the experiments carried out in this thesis was performed on T115 GBM case. T84 and T146 (along with T115) were used in pERK and Edu assays, expanded later on in this section.

2.2. Culturing Primary Patient-derived GBM Cell Lines

GBM tumour samples were collected from patients undergoing surgical resection at Auckland City Hospital and was processed in accordance with the cancer cell isolation method established in our lab (Park et al., 2022). Briefly, the tumour tissue was diced into smaller fragments for enzymatic dissociation. From this, the cell mix was filtered using a cell strainer and centrifuged before seeding into a T75 culture flask containing GBM cell media [that is formulated by DMEM/F12 (Gibco), 2% B27 without vitamin A (Invitrogen), 1% penicillin-streptomycin (Gibco) and 1% GlutaMAX (Invitrogen)] for overnight incubation at 37ºC. The next day, cells that did not adhere to the flask were isolated again for centrifugation and resuspended into a new culture flask containing culture medium. The

primary GBM case used in this thesis (T115) grew as spheroids. When these spheres reached roughly 300 μm in diameter, Accutase (Invitrogen) solution was used to separate the cells into single cells for passaging or plating for future experimentation.

2.2.1 **Maintenance of primary patient-derived GBM Cell Lines**

Media changes were conducted every 2-3 days, where half of the GBM media in the culture flasks was removed for centrifugation to separate the supernatant/media from the cell pellet. The supernatant was discarded, and the pellet was resuspended using the same volume of cell media removed before re-introducing the mix into the culture flask before incubation at 37ºC with 95% air and 5% CO2.

Aforementioned, when the culture flask reaches roughly 90-95% confluency (when spheres reach roughly 300 μm in diameter), the cells were harvested for passaging to ensure the tumour cells were "healthy". The procedure begins with the removal of all media from the culture flask and into a 50 mL Falcon tube. 3 mL of Accutase was added to the flask and placed in the incubator for 5 minutes to enable cell detachment. During this period, the media containing free-floating GBM tumour cells was centrifuged at 1000 revolutions per minute (RPM) for 5 minutes. After the incubation with Accutase, the flask was firmly tapped along the sides to ensure the majority of the cells had detached from the base of the flask and a quick inspection to confirm detachment was conducted using a light microscope. Following centrifugation, the supernatant was removed and placed within a 15 mL falcon tube, labelled Condition Media and was set aside for use later. The Accutase and cell mix from the culture flask were transferred into the spun falcon tube containing a pellet of GBM cells. Depending on the tumour morphology, additional steps were taken to ensure successful cell detachment. For tumour spheres (such as T115), the flask was washed down with an additional 3 mL of Accutase to ensure nearly all the cells were harvested. Following this, all the media present in the flask was isolated and placed within the spun-down falcon. Then the tube was gently titrated to break the pellet of cells at the bottom and carefully swirled in a 37°C water bath for a duration of 5 minutes. From this point, both tumour sphere and tumour monolayer cells (that is T84 and T146) share the same passaging procedure where 6 mL of stem cell media, excluding supplementary growth factors and Heparin, was added to the falcon tube, before being titrated and centrifuged for 5 minutes at 1000 RPM. Thereafter, the supernatant was discarded, and the pellet was resuspended in 5 mL of growth factor and heparin

supplemented stem cell media. Cell count was conducted using Trypan Blue Solution (ThermoFisher Scientific).

Before plating, around 2 million cells of each case was reseeded into a new T75 flask containing 5 mL of GF media (including supplementary growth factors and heparin) and 5 mL of condition media to support the formation of a new generation of GBM cells.

2.2.2 **Monolayer Cell Plating**

Following reseeding, the required cell volume for plating was diluted into a freshly made growth factor supplemented stem-cell media (containing heparin, EGF and FGF, (PeproTech)) and plated at roughly 5,000 viable cells per well in Matrigel® (Corning) coated 96-well plates. These plates were incubated at 37ºC with 96% air and 5% CO2 for 48 hours prior to experimentation. Monolayer cell plating was conducted for migratory biomarker characterisation experiments.

2.2.3 **Tumour-Spheroid Plating**

For the formation of tumour spheres appropriate for live cell migrations studies, the cells were further diluted by the same volume of growth factor media to bring the cell count to 2,500 viable cells per well. From this cell mixture, 100 μL was then plated into special sphere-forming 96-well plates (Thermo Fisher Scientific) to stimulate spheroid formation. These plates achieved this as they lacked a flat bottom and prevented tumour cells from adhering to the base and remain free-floating in the wells. The “U”-shaped well design enabled tumour cells to adhere to each other and form a sphere. Similar to monolayer cell plating, these plates were also incubated for 48 hours at 37ºC with 95% air and 5% CO2.

Following the incubation period, the tumour spheres were examined under a light microscope to verify successful tumour sphere formation. Tumour spheres were extracted and transferred into relevant 24-, 48- and 6- well Matrigel-coated plates for various experiments. A 10-100 μL pipette was used to transfer the spheres as 15 μL droplets to the base of the Matrigel-coated wells. Utmost care was taken when transferring spheres, especially for those used in live cell imaging as a broken sphere would not migrate evenly from all sides. The plates containing the spheres were incubated for approximately 2-3 hours at 37ºC with 95% air and 5% CO2 for successful sphere adherences. Afterwards, each plate was carefully topped with

relative volumes of migratory media (that consists of growth factor media with 1% FBS (Moregate)) ready for drug treatment. Note: these cells are referred as spheroid cells throughout the thesis.

2.3. 5-ethynyl-2'-deoxyuridine (EdU) proliferation Assay

5-ethynyl-2'-deoxyuridine (EdU; 10 μM Invitrogen) was added to the GBM cultures 24 hours prior to fixation to determine cell proliferation. Cells were fixed in 4% paraformaldehyde (PFA; Scharlau) for 15 minutes, and EdU was visualised via manufacturer's instructions. Cell nuclei were counterstained for 20 minutes with Hoechst 33258 (Sigma-Aldrich) diluted 1:500 in PBS. The percentage of EdU positive cells was obtained via the automated fluorescence microscope ImageXpress® Micro XLS (Molecule Devices) and the cell scoring journal on MetaXpress® software (Molecule Devices). The IC50 values were estimated from the concentration-response curve where the concentration of each compound was plotted against the percentage of EdU-positive cells normalised to the vehicle (0.01% DMSO) (variable response, three parameters). Data shown are from at least four independent GBM cases. The non-linear curve and IC50 estimates were produced in Prism GraphPad Software. This assay was conducted by Elizabeth A. Cooper on my behalf.

2.4. pERK Assay

To determine an appropriate concentration of Trametinib and U0126, a pERK assay was conducted. Briefly, T115, T146 and T84 patient-derived GBM cells were treated with up to 100 μM of Trametinib, U0126 and vehicle (0.01% DMSO) for 30 minutes, 1 hour, 2 hours and 48 hours.

The mean integrated intensity of pERK was measured via the automated fluorescence microscope ImageXpress® Micro XLS (Molecule Devices) and quantified using the cell scoring journal on MetaXpress® software (Molecule Devices). The mean integrated intensity of pERK was plotted against the range of concentration of Trametinib and U0126 along with vehicle (0.01% DMSO) and IC50 values were extrapolated following fitting of a non-linear curve on Prism GraphPad Software. This assay was conducted by Elizabeth A. Cooper on my behalf.

Table 3 List of antibodies and their relative dilutions used for pERK Assay

Antibody	Species	Company	Catalogue	Dilution
pERK	Rabbit	Cell signalling	9371L	1:500
Hoechst	-	Sigma-Aldrich	33258	1:500

2.5. Drug Treatment

Prior to any drug addition, all plates had undergone a half media change where half of the media volume was replaced with fresh GF media, for instance 50 μL per well in a 96-well plate.

MEK inhibitors, Trametinib (Selleckchem) and U0126 (Cell Signalling), along with the vehicle, Dimethyl Sulfoxide, (DMSO; Sigma-Aldrich), were used in all drug-treated experiments. The stock concentrations of both MEK inhibitors (trametinib and U0126) were determined based on the IC_{50} values of pERK and EdU outputs, which were 100nM and 1 μM, respectively. These working stocks were further diluted by 1:1000 in migratory media before being added to each plate so that the final concentration of the MEK inhibitors matched their respective IC_{50} values stated above (figure 1).

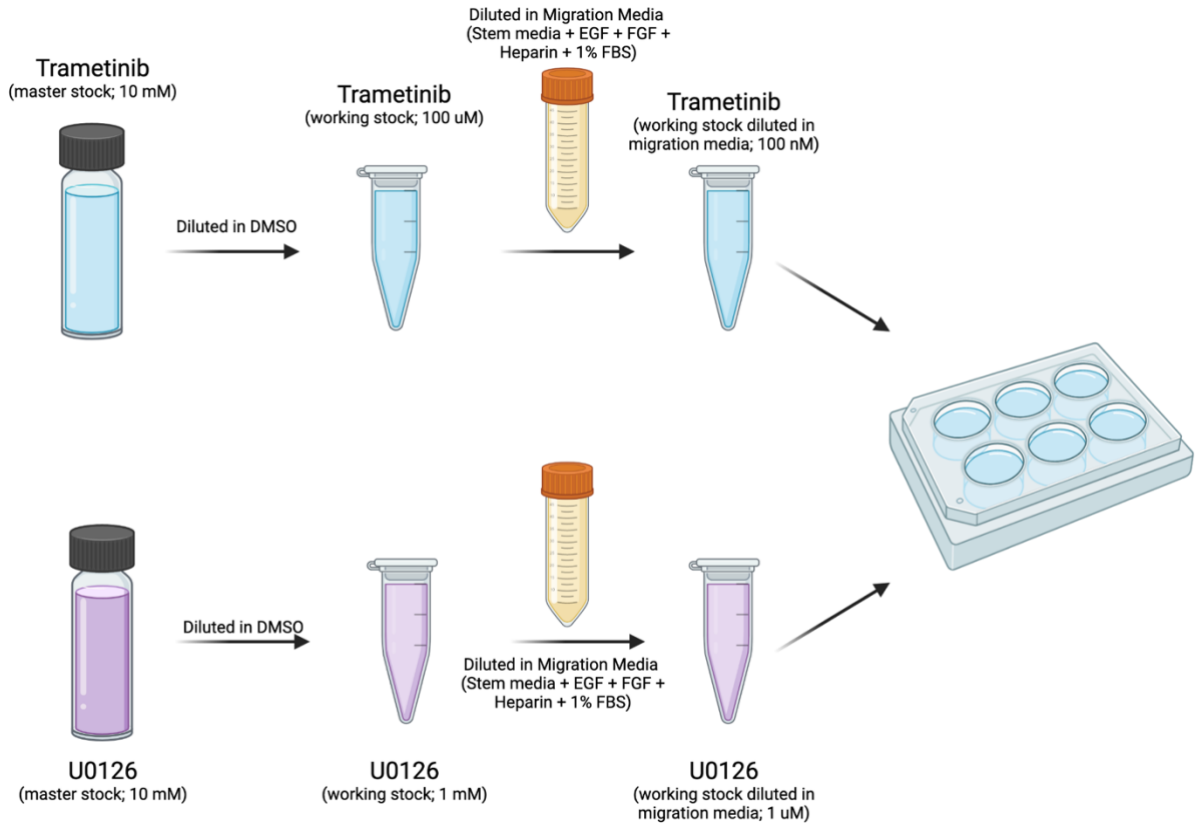

Figure 1. Serial dilution of MEK inhibitors trametinib and UO126 to produce a suitable working concentration.

2.6. Immunocytochemistry (ICC)

48 hours following the addition of MEK inhibitors, characterisation plates (96-well plate with cells in a monolayer fashion and 48-well plate with cells in spheroid morphology) were fixed with 8% PFA for 15 minutes to allow cell permeabilization. The washing regimen (consisting of washing the cells with PBS-T thrice for 10 minutes on a mechanical rocker) was performed. Subsequently, primary antibodies combination (table 4) diluted in immunobuffer containing 1% goat serum, 0.2% Triton X-100 and 0.04% Thiomersal in PBS was added into relevant wells and incubated overnight at 4°C.

After incubation, the washing regimen was carried out. Fluorophore-conjugated antibodies (dubbed secondaries, table 5) were diluted in the same immunobuffer mentioned before and added to the plate for another overnight incubation at 4°C wrapped in foil. The next day after a single wash of cells, Hoechst 33258 (Sigma-Aldrich) was introduced to the plate for 30 minutes to stain the nucleus. The plate was washed twice afterwards and topped with PBS-T containing 0.04% Proclin (Sigma-Aldrich) and imaged right away or stored at -20°C for future analysis.

Table 4 List of antibodies and their relative dilutions used for immunocytochemistry

Antibody	Species	Company	Catalogue	Dilution
Cleaved caspase 3	Rabbit	Cell signalling	CS9661	1:500
pFAK (phosphor Y397)	Rabbit	Abcam	AB81293	1:500
Ki67	Mouse	Dako	M7240	1:500
MMP-9	Rabbit	Abcam	AB38906	1:500
NCAM	Mouse	Santa Cruz	SC7326	1:500
PSA-NCAM	Mouse	Absolute Antibodies	Ab00240-2.0	1:500
PST	Rabbit	Thermofisher	PA5-26774	1:500
STX	Rabbit	Abcam	AB155115	1:1000

Table 5 List of fluorophore-conjugated antibodies plus Hoechst and their relative dilutions used for immunocytochemistry

Fluorophore-conjugated antibodies	Species	Company	Catalogue	Dilution
Goat anti-mouse Alexa Flour® 488	Mouse	Invitrogen	A11034	1:500
Goat anti-rabbit Alexa Flour® 594	Rabbit	Invitrogen	A11012	1:500
Hoechst	-	Sigma-Aldrich	33258	1:500

2.7. Image Acquisition And Analysis

Image acquisition for both ICC monolayer and ICC spheres was conducted using ImageXpress® Micro XLS system that contained an automated fluorescence microscope (Molecular Devices, CA, USA). Specifically, the 10× CFI Super Plan Fluor ELWD ADM objective lens and Lumencor Spectra X configurable light engine source was used in the acquisition. The excitation and emission filters, DAPI, FITC and TRED were utilised to

observed different markers of migration and proliferation (table 6). The exposure was optimised for each antibody and maintained across the experimental repeats.

Table 6 Excitation and emission filter parameters used for ImageXpress Micro XLS

Cube	Filter	Lumencor Light Engine	Excitation range	Excitation peak	Dichoric	Emission range	Emission peak
Quad 5	DAPI	UV (380-410)	381-399	390/18	436	445-469	457
Quad 5	FITC	Cyan (460-490)	484-504	494/20	514	518-542	530
Quad 5	TRED	Green (535-600)	561-590	575/25	604	612-643	628

2.7.1 **Monolayer analysis**

The high-throughput images acquired from the 96-well plate containing cells in a monolayer morphology was analysed using multi-wavelength cell scoring module available on the MetaXpress® software (Molecular Devices) to quantify the cell number and staining intensity of markers in the presence MEK inhibitors and vehicle. For CC3 and Ki67, positive cells associated with a nucleus (Hoechst-positive) were used for quantification and the percentage of cells stained positively for Ki67 or CC3 out of the total cell present was given as an output. For the other markers, the integrated intensity per cell was taken into consideration, as more appropriately reflected cellular changes in the presence of MEK inhibitors. Generally, the staining observed is either nuclear or cytoplasmic. A threshold is set for the signalling intensity of the pixels above background levels and below brightly labelled debris. The integrated intensity for the marker of interest is determined via subtracting the background noise and excluding the debris. The mean intensity for each marker of interest is the summation of the number of pixels above background and the intensity of those pixels minus the background divided by the total cell number (denoted by the number of Hoechst-positive cells). For each analysis, the settings were optimized for each antibody combination and randomly tested on four images to ensure quantification was reflective of the actual staining. The data obtained is an average of the four images taken from each well, but the data presented is normalised so that comparisons between two repeats can be conducted.

2.7.2 **Spheroid Analysis**

The spheroid images was obtained via ImageXpress® Micro XLS system and resulted in small individual images of the sphere as the imaging system was limited in its ability to image the whole sphere without losing resolution. Each segmented image of the sphere was montaged into a larger image on the MetaXpress® software. After this, each sphere file was opened in Fiji (distribution of ImageJ, (Schindelin et al., 2012)) to find the centre of the sphere for masking because the purpose of this experimentation was to investigate the changes in the intensity of markers of interest in the presence of MEK inhibitors. A special script, ROI centre was ran to produce an automated outline of the centre of the sphere and followed by another script, ROI centre to remove the centre of the tumoursphere, leaving on the region of interest (that is the individuals cells that have migrated out from tumoursphere core). This was repeated for all three channels (DAPI, FITC, TRED) across all three treatment conditions. Markers of interest formulated in the mouse species were represented by the FITC channel and markers of interest formulated in the rabbit species were represented by the TRED channel (table 4).

After masking the tumour core, the output files were transferred to ZEN microscopy software (Zeiss) for analysis where the 3 channel ROI analysis setting was utilised. A parameter box was created around the tumoursphere and the immediate surroundings so that the analysis was limited to this region. An automated threshold was placed and highlighted all of the bright spots present in the file (these are our individual migrating cells). Each channel was examined individually to visually determine the threshold on the migrating cells with a three sigma threshold used for FITC channel and an otsu threshold used for TRED channel. Cells that were dark or did not have enough difference between themselves and the background were ignored in the automated thresholding. This meant that data is comparable across all the images in the dataset. In the end, data output demonstrated area of the individual migrated tumour cells ($pixel^2$) and intensity mean of each tumour cell (gray). This analysis was conducted by Richard Yulo from BIRU.

2.8. Live Cell Migration

2.8.1 **Live Cell Imaging**

Following the drug treatments, the 24-well plate was transferred into a temperature and CO_2 controlled Live Cell Microscope Incubator (Ziess XL-3 stage incubation chamber). The

chamber was fitted with an Axiovert 200 M motorised inverted microscope and an Axiocam MRm digital camera (Zeiss). The temperature and CO_2 levels of the chamber were kept consistent at 37°C and 5%, respectively. The microscope magnification at 10× with 0.25 bright-field images was obtained every 20 minutes using the AxioVision program and the imaging suite (Zeiss). To ensure clear distinctions and focus on migrating cells from the tumour core, colour and exposure settings were set to black and white. These setting parameters were maintained across all three repeats.

2.8.2 **Tumour sphere migration analysis**

Images obtained from the live cell migration were sent to our collaborators at the Biomedical Engineering Facility for tumour sphere migration analysis. The analysis parameters were established by Chun Kiet Vong and the manuscript is currently in preparation. The Finite element analysis part of the Continuum Mechanics, Image analysis, Signal processing and system identification software (CMISS) was used for migration analysis since Chun has demonstrated the robust measurement of migration in a spheroid assay. The analysis system begins with the division of the sphere shape into a finite number of smaller elements for efficient and effective mathematical solving. A mesh of smaller elements is produced as a result. Then, the shape change is determined by material properties, loading and fixation conditions, degrees of freedom and potential environmental conditions. Appropriate equations for the model were applied. Following this, the previously defined equations were solved and the result describes the change via determining the displacement of the nodes in the mesh as it changes over time. Visualisation and data analysis completed the process.

To the live cell images, machine-learning algorithm designates boundaries around the sphere and the migrating region in ImageJ. Then, the images were threshold and despeckled till only the drawn boundary was left, and these threshold images were converted into a text image file in ImageJ before transferring to CMISS where mesh fitting was conducted. Following mesh fitting and checks, meshes from different time points were selected and the displacement of each node was calculated producing a file containing the displacements over time data. Lastly, the migration rate was calculated from the node displacement file via maximum principal strain analysis in CMISS.

2.9. Quantitative real time-polymerase chain reaction (qRT-PCR)

Tumour spheroids were plated into a 6-well plate topped with growth factor media and treated with either MEK inhibitor or DMSO (control), and incubated for a 48-hour period. Before RNA extraction was implemented, the viability of the cells was examined under a light microscope. The cells were lysed using the RNAqueous kit where all media was removed, and 100 μL of RNA lysis buffer was added before cells were scraped thoroughly and triturated. The cell lysate was collected in a sterile 1.5 mL conical screw cap tube (Axygen). Subsequent RNA was isolation was conducted in accordance to the manufacturer's instructions. The quantity and quality of isolated RNA was determined using the Nanodrop (Thermofisher Scientific). Samples with 260/280 and 260/230 ratios lower than 1.5 were cleaned via rewashing. Subsequently, cDNA was synthesised using Superscript IV First-strand Synthesis cDNA kit in accordance with the manufacturer's instructions. The concentration of cDNA varied as it was dependent on the RNA isolated from each condition. Quantitative real-time PCR was implemented with SYBR Green qPCR SuperMix-UDG and ROX (Invitrogen) using QuantStudio 12K Flex Real Time PCR System (Thermofisher Scientific). Gene expressed was quantified relative to the expression of housekeeping gene β Actin and RPL-30, which encoded beta-actin protein and ribosomal L30E protein (component of 60S subunit forming ribosomes) respectively via the $2^{-\Delta\Delta Ct}$ method (Livak & Schmittgen, 2001).

Table 7 List of primers used for qRT-PCR

Gene	Protein		Sequence (5' to 3')	Amplicon (base pairs)
ACTB	β Actin	Fw	TGGTGGGCATGGGTCAGAAGGA	94
		Rv	ATGCCGTGCTCGATGGGGTACT	
BAX	BAX (Bcl-2 Associated X-protein)	Fw	GCCCTTTTCTACTTTGCCAGC	94
		Rv	AGTCCAATGTCCAGCCCATG	

BCL2	BCL2	Fw	ACTGGGGGAGGATTGTGGCCTT	70
		Rv	ATCTCCCGGTTGACGCTCTCCA	
JUN	c-Jun	Fw	ACGGCCAACATGCTCAGGGA	89
		Rv	TGCGTTAGCATGAGTTGGCACCC	
CREB	CREB (cAMP-response element binding protein)	Fw	AGCCGAGAACCAGCAGAGTGGA	86
		Rv	TGGCAATCTGTGGCTGGGCT	
DCX	Doublecortin	Fw	ATGCCCCTGAGCAAGTCGAGGA	78
		Rv	CGGTGCCTCCATTTACACGAGCA	
PTK2	FAK	Fw	AGAAGAAAAGAATTGGGCGGA	135
		Rv	GGCTTGACACCCTCGTTGTA	
LGALS1	Galectin 1	Fw	ATCATGGCTTGTGGTCTGGT	20
		Rv	GCACAGGTTGTTGCTGTCTT	
MKI67	Ki67	Fw	AGCGGAAGCTGGACGCAGAA	79
		Rv	TCCAGGGGTTGGGCCTTTTCCT	
L1CAM	L1 protein (L1 cell adhesion molecule protein)	Fw	ATCATCCTCCTGCTCCTCGT	88
		Rv	TGTCACTGTACTCGCCGAAG	
MMP9	Matrix metalloproteinase 9 (MMP-9)	Fw	ATGTACCGCTTCACTGAGGG	
		Rv	GTTCAGGGCGAGGACCATAG	82

NCAM	NCAM	Fw	TCAGTGGTGTGGAATGATGATTC	89
		Rv	CCGGCGTCGTCGATGT	
NES	Nestin	Fw	AGCTGGCGCACCTCAAGATGTC	89
		Rv	AGGTGTTTGCAGCCGGGAGTT	
ST8Sia IV	PST	Fw	GAGCAGTTTTAAGCCTGGTGATG	84
		Rv	TAGGAGGCTATGTAGATCATGAGAAATG	
RPL-30	60S ribosomal protein L30	Fw	TACGTCCTGGGGTACAAGCA	86
		Rv	AAAGCTGGGCAGTTGTTAGC	
SOX2	SOX2	Fw	ACAGCATGTCCTACTCGCAG	70
		Rv	GACTTGACCACCGAACCCAT	
ST8Sia II	STX	Fw	GCTGACCAACAAAGTCCACATC	108
		Rv	GAAACGTGTGGCCAGGGTAT	
TP53	Tumour protein p53 (p53)	Fw	CTGGCCCCTGTCATCTTCTG	131
		Rv	ACATCTTGTTGAGGGCAGGG	

2.10. Western Blotting

Similar to qRT-PCR, tumour spheroids were plated into a 6-well plate topped with growth factor media and treated with either MEK inhibitor or DMSO (control) and incubated for a 48-hour period. Before protein extraction was implemented, the viability of the cells was examined under a light microscope. Following this, media was removed and 100 μL of RIPA buffer (150mM NaCL, 0.1% Triton, 0.5% deoxycholate, 0.1% SDS and 50mM Tris-HCL, pH 8) plus mini proteasomal cocktail inhibitor (Sigma-Aldrich) was added for cell scraping and cell lysate trituration. The lysate was collected in a sterile 1.5 mL conical screw cap tube (Axygen) and placed on ice before this step was repeated for the other conditions. All the lysate tubes were placed within the Next Advance Bullet Blender for 5 minutes at level 4 for further cell homogenization.

Protein concentration within each lysate was quantified using a BSA standard curve produced in accordance with the Biorad DC Protein Assay kit instructions. The BSA standard curve absorbance was read at 750 nm via the BMG FLUOstar OPTIMA microplate reader.

Following quantification, protein samples were diluted with Laemmli Sample Buffer (4x) (Sigma-Alrich) and RIPA buffer to obtain a final concentration of 30 ug per well within NuPage 4-12% Bis-Tris SDS-Page protein Gels (Invitrogen) when loaded. The same protein samples were loaded into the two gels and ran with 1x NuPage MES SDS running buffer solution (Invitrogen) at 100V for 30 minutes followed by an hour at 150V within a gel tank. Subsequently, the protein samples (within the gel) was transferred onto an Immobilon-FL PDVF membrane (Millipore, MA, USA) via a Trans-Blot Cell module (BioRad) with NuPage transfer buffer (5% MeOH) at 100V for 2 hours. After briefly drying, the membranes were snipped at the top right corner before incubation with primary antibody solutions (table 8) that were diluted in 1:1 Intercept blocking buffer (Licor) and Tris-buffered saline with 0.1% Tween 20 (TBS-T) under dark conditions overnight at 4°C. The next day, primary antibodies were removed and the membranes were washed thrice using TBS-T solution for 10 minutes each on an orbital shaker. Afterwards, the membranes were subjected to secondary antibody incubation (table 8), where the fluorophore-conjugated antibodies were diluted 1:1 with Intercept blocking buffer and TBS-T under dark conditions for 3 hours at room temperature. Both membranes were washed again and left to dry at least an hour before imaging. Membranes were imaged using the LiCOR Odyssey® Fc Imaging System and

quantified via LiCOR Image Studio Lite along with normalisation with the housekeeping protein, β Actin.

Table 8 List of primary and secondary antibodies used for Western Blot

Antibody	*Species*	*Company*	*Catalogue*	*Dilution*
β Actin	Mouse	Abcam	AB276	1:5000
β Actin	Rabbit	Abcam	AB75186	1:5000
NCAM	Mouse	Santa Cruz	SC7326	1:500
PSA-NCAM	Rabbit	Absolute Antibodies	Ab00240-23.0	1:500
MMP-9	Rabbit	Abcam	AB38906	1:500
Goat anti-mouse IRDye® 680LT	-	LiCOR	926-68020	1:10,000
Goat anti-rabbit IRDye® 800CW	-	LiCOR	926-32211	1:10,000

2.11. Statistical Analysis

Statistical analysis was conducted using GraphPad Prism 8 (GraphPad Software Inc.). All graphs displayed contain means ± standard error of measurements (SEM), excluding the pERK and EdU graphs which contain means ± standard deviation (SD). Statistical significance was set at $p < 0.05$ and One-way ANOVA with Dunnett's post-test was utilised for ICC monolayer, ICC sphere and western blot assays. In addition, two-way ANOVA followed by Tukey's post-test was completed for live cell migration.

Chapter 3. Results

3.1. Establishing an appropriate concentration of MEK inhibitors

To explore the potential reduction in proliferation within GBM cells, MEK inhibitors, U0126 and trametinib, were utilised throughout this thesis. U0126 and trametinib are MEK-1 and MEK-2 subset-specific inhibitors leading to the cessation of ERK phosphorylation and altering downstream proliferation and migration signalling (Chappell et al., 2011; Guo et al., 2020).

Firstly, a concentration- and time-response curve was conducted to determine an appropriate concentration of U0126 and trametinib that affected proliferation and had minimal toxicity. A range of U0126 and trametinib concentrations were spiked into three patient-derived GBM cases; T146, T115 and T84 (n = 3) and the expression of phosphorylated ERK (pERK) was used as a validation tool. The mean cytoplasmic integrated intensity of pERK of both MEK inhibitor concentrations was compared with the vehicle, 0.01% DMSO.

A concentration-dependent relation was observed between pERK and the MEK inhibitors, where phosphorylation of ERK diminished as the concentration of U0126 and trametinib increased (figure 2, A). Specifically, the data obtained post-1 hour treatment demonstrated that trametinib was a more effective inhibitor against MEK than U0126. This is because the phosphorylation of ERK dramatically decreased in the presence of trametinib and almost completely abolished at 1 μM of trametinib (figure 2). On the contrary, U0126 required a higher concentration to achieve similar effects as trametinib, as shown by the IC_{50} value. The IC_{50} represents half of the maximal inhibitory concentration of the drug based on the normalised mean integrated intensity of pERK. The IC50 for trametinib is roughly 100 nM, while the IC_{50} for U0126 is 10 μM.

Similar to the pERK assay, three patient-derived GBM cases, T146, T115, and T84, were treated with various concentrations of trametinib and U0126, and their mitotic activity was investigated via EdU cell proliferation assay (n = 3). Proliferation was quantified by the percentage of cells positively stained with EdU relative to vehicle 0.01% DMSO.

A dramatic decrease in the proliferative activity was observed when cells were treated with trametinib over 48 hours, as indicated by a substantial decrease in EdU positive cells. The

IC50 for trametinib determined from the Edu assay data is roughly 100 μM. On the other hand, the proliferative activity when cells were treated with U0126 gradually decreased the percentage of Edu-positive cells over 48 hours (figure 2, B). The IC_{50} value for U0126 is 1 μM. The proliferation levels for U0126 are ten times lower than for trametinib. Based on these findings, the rest of the experimentations were consistently carried out using 100 nM of trametinib and 1 μM of U0126.

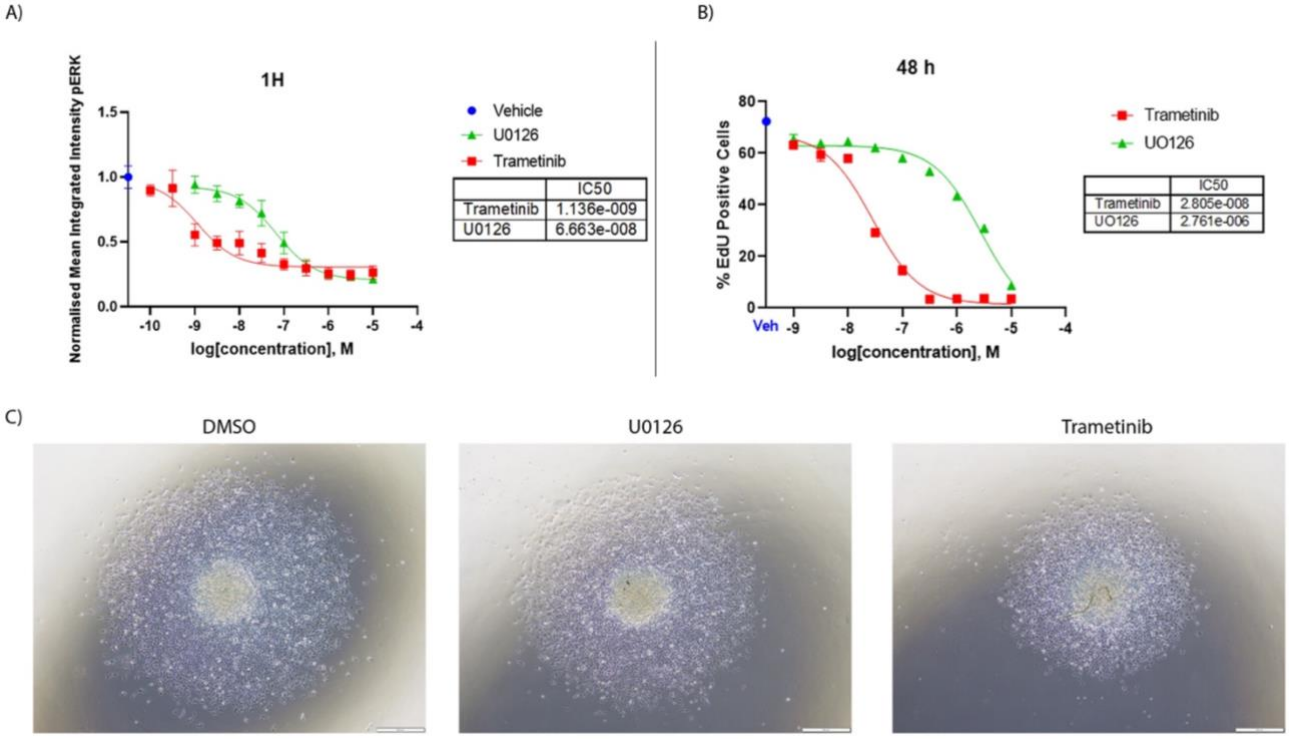

Figure 2. Concentration-dependent response of phosphorylated ERK and of EdU-positive cells in patient-derived GBM stem cells.

(A) A concentration-response curve was to determine the IC50 of each inhibitor on the basis of phosphorylated ERK signalling. Three different patient-derived GBM cell lines were treated with a gradient of concentrations of trametinib (red), U0126 (green) and a single concentration vehicle DMSO (dark blue) for 30 minutes, 1 hour, 2 hours and 48 hours (n = 3). The mean pERK cytoplasmic integrated intensity was normalised to the vehicle (0.01% DMSO). (B) A concentration-response curve to determine the effects of trametinib and U0126 on the proliferation activity of GBM cells. Three different patient-derived GBM cell lines were treated with a various concentrations of trametinib (red), U0126 (green) and a single concentration of vehicle DMSO (dark blue) for 48 hours (n = 3). The percentage of EdU-positive cells was normalised to its vehicle (0.01% DMSO). (C) Light microscope images of tumourspheres after 96-hour live cell migration experiment where tumourspheres were incubation with trametinib, U0126 and 0.01% DMSO (control). Concentration-response data were obtained from Elizabeth Cooper. Scale bar = 500 μm.

3.2. Exploring the effects of MEK inhibitors upon cell proliferation and cell death in patient-derived GBM cells

Using the concentration determined above, the effects of trametinib and U0126 upon cell death were investigated using cleaved caspase-3 (CC3), a well-characterised apoptosis marker (Dull et al., 2018) to potentially observe apoptotic cell death stimulated by either MEK inhibitor. After adding of 100 nM of trametinib and 1 μM of U0126 to T115 cells plated in ICC characterisation plates, the percentage of cells staining positive for CC3 was determined before normalisation with the control, 0.01% DMSO treated cells. A one-way ANOVA was conducted along with the Dunnet post-hoc test to determine any statistical difference across two repeats of T115.

The data shown in figure 3 demonstrated a significant reduction in CC3 staining when treated with both U0126 (~0.8%, $p < 0.01$) and trametinib (~0.6%, $p < 0.0001$) when compared to the control, 0.01% DMSO. Overall, the respective concentrations of trametinib and U0126 do not yield high amounts of apoptotic cell death. This gave us the confidence that any possible inhibitory effect observed will most likely be due to the drugs binding and blocking MEK1 and MEK2 subsets.

The effect of MEK inhibitors on the proliferation activity was determined again, but this time utilised Ki67, a well-established proliferative marker (X. Sun & Kaufman, 2018). Ki67 demonstrated a significant decrease in staining when treated with both U0126 (~0.7%, $p < 0.01$) and trametinib (~0.4%, $p < 0.0001$) when compared to the control, 0.01% DMSO (figure 3, C).

Overall, both CC3 and Ki67 staining significantly decreased in the presence of trametinib in contrast to the control, DMSO. U0126 treated cells also exhibited a reduction in CC3 and Ki67 signalling. However, the most noticeable reduction was trametinib, as seen in figure 3, A. There was no significant difference between trametinib and U0126 in either CC3 or Ki67 signalling.

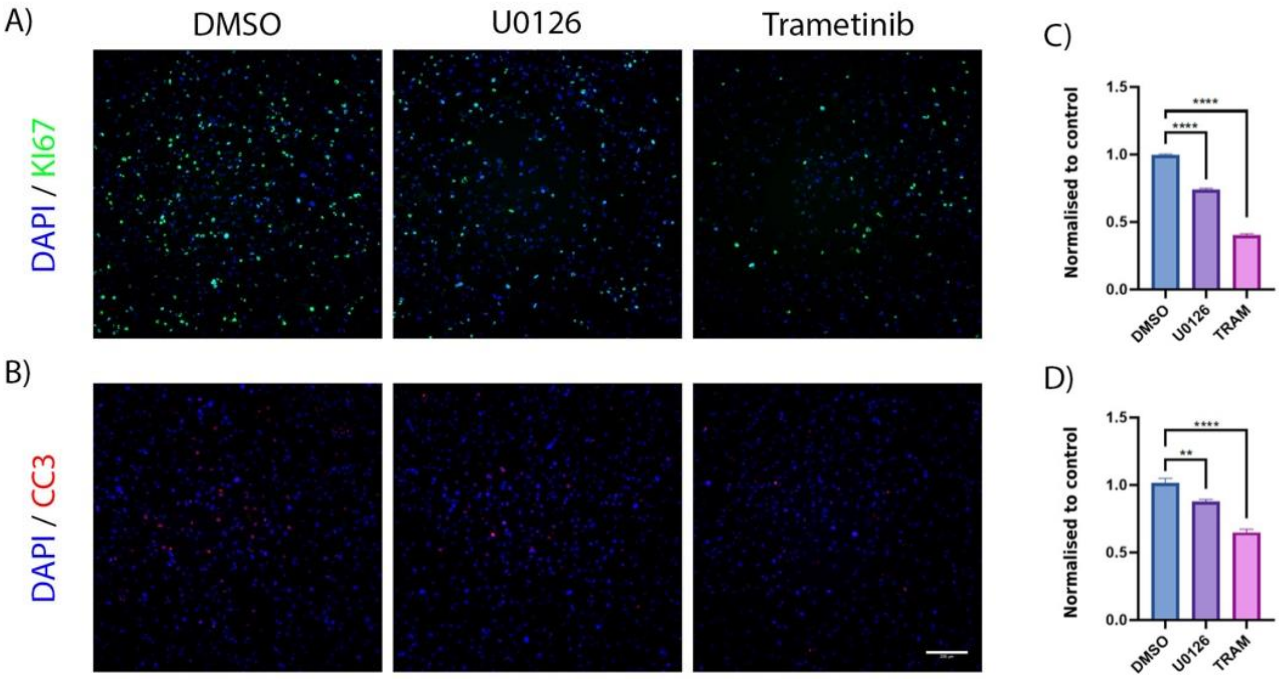

Figure 3. The effects of MEK inhibitors on Ki67 and CC3 signalling. T115 GBM cells were incubated with 100 nM trametinib or 1 μM U0126 or control (0.01% DMSO) for 48 hours.

(A-B) Representative images of Ki67 and CC3 signalling in the presence of either MEK inhibitor and control (DMSO) in T115.19 repeat. (C-D) The percentage of Ki67 positive cells and the percentage of CC3 positive cells was normalised to the control (0.01% DMSO). * $p < 0.05$, ** $p < 0.01$, *** $p < 0.001$, **** $p < 0.0001$ significance relative to control (DMSO) via one-way ANOVA and Dunnet post-hoc test. *n* = 3 repeats of T115, scale bar = 200 μm.

3.3. Investigating the effects of MEK inhibitors upon cell migration in patient-derived GBM cells

I next explored the effect of MEK inhibition on tumour cell migration. A comprehensive gene expression analysis was conducted using qRT-PCR, which included cell survival, proliferation, and migratory markers. Their protein expression was subsequently followed by high-throughput ICC experimentations and some markers were validated via western blotting.

After T115 tumourspheres were incubated for 48 hours with 1 μM of U0126 and 100 nM of trametinib as well as 0.01% DMSO (control), the mRNA was extracted and turned into cDNA for qRT-PCR. In total, roughly 50 ng/μL of cDNA was created and each gene was allocated roughly 13 ng/μL of cDNA across all three conditions. Migratory genes including *NCAM*, *ST8Sia II*, *ST8Sia IV*, *L1CAM*, *PTK2*, *LGALS1*, *MMP-9*, and *DCX* were chosen to be screened alongside proliferative, apoptotic and cell cycle-associated genes such as *MKI67*, *SOX2*, *BAX*, *BCL2*, *CREB*, *JUN*, *TP53*, and *NES*. qRT-PCR data were normalised to β actin and RPL-30 signal respectively, and analysed using the $2^{-\Delta\Delta Ct}$ method (Livak & Schmittgen, 2001). Data is presented as individual repeats of T115 ($n = 3$) relative to control, DMSO (set to the value of 1), as well as integration of all three repeats of T115 (figure 4, B).

Across the three repeats of T115 tumourspheres, a prominent trend in gene expression emerged. When tumourspheres were treated with trametinib, a substantial four-fold increase in *NCAM* and a near three-fold increase in *STX* appeared. On the contrary, a strong eight-fold decrease in *MMP-9* and a near four-fold decrease in *PST* were also observed. It is important to note that a strong increase or decrease in gene expression does not translate into a higher or lower protein expression downstream but, offers grounds for further protein analysis.

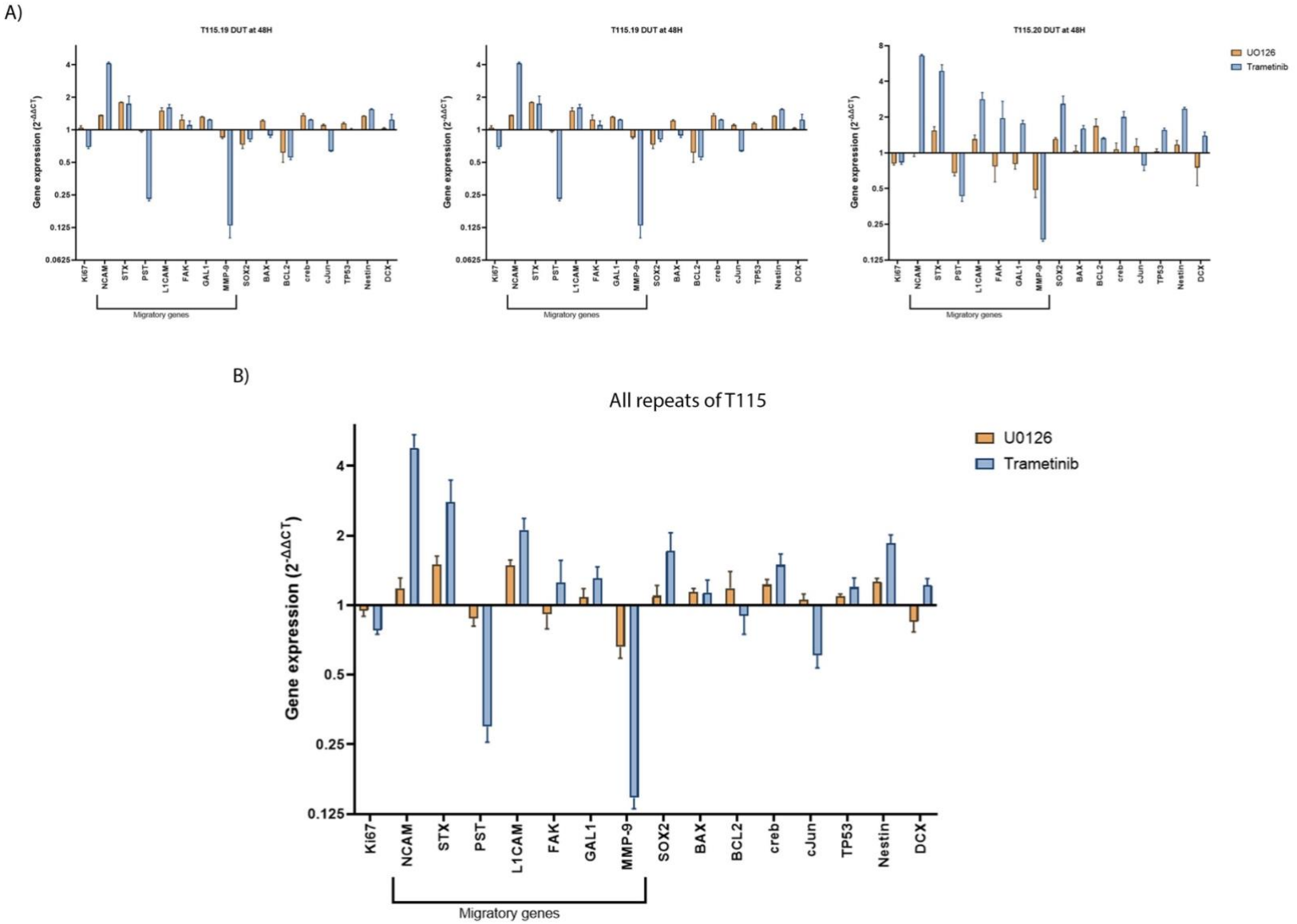

Figure 4. Treatment of GBM with MEK inhibitors trametinib and U0126 alters migration associated gene expression.

T115 GBM tumourspheres were treated with 100 nM trametinib or 1 μM U0126 or control (0.01% DMSO) for 48 hours to investigate changes in gene expression due to MEK inhibitors. (A) Individual repeats of T115 treated with MEK inhibitors demonstrate a potential trend in gene expression. (B) All three repeats of T115 complied into a single graph to observe the changes in gene expression when treated with MEK inhibitors. *n* = 3 repeats of T115**.**

Migratory markers including NCAM, PSA-NCAM, STX, PST, MMP-9, and pFAK were investigated in two distinct cell models, monolayer and spheroid, since the monolayer configuration lacks three-dimensional morphology but serves as a high-throughput screening tool while tumourspheres closely resembles tumour cell morphology within the brain. ICC experiments on monolayer patient-derived cells were conducted on one patient-derived GBM case, T115, and repeated thrice ($n = 3$). Similarly, ICC experiments on tumoursphere patient-derived cells were conducted on the T115 case and repeated twice ($n = 2$).

Initially, the characterisation of migratory markers in GBM was conducted via ICC on T115 cells that exhibited a monolayer morphology. The presence of the MEK inhibitors produced variable results on the migratory markers. For instance, treatment of trametinib produced an increase in the mean cytoplasmic integrated intensity of NCAM compared to control (0.01% DMSO) ($p < 0.0001$) (integrated intensity detailed in subsection 2.7.1). Similarly, the mean integrated intensity of phosphorylated FAK, PSA-NCAM, PST and MMP-9 markers also increased when T115 cells were treated with trametinib compared to control ($p < 0.001$, $p < 0.01$, $p < 0.05$ and $p > 0.05$, respectively). On the contrary, the mean integrated intensity of STX was reduced in trametinib-treated cells compared to control ($p > 0.05$).

On the other hand, the mean integrated intensity of NCAM, PSA-NCAM, PST, and MMP-9 in U0126 treated cells remained roughly on par with the mean integrated intensity of the markers when treated with control (0.01% DMSO). However, this finding is not statistically significant. Interestingly, the mean integrated intensity of STX increased in U0126 treated cells when compared to control ($p <0.01$). Another migratory marker that exhibited this trend is phosphorylated FAK which increased in the presence of U0126 in contrast to control; however, as the p-value of this finding was greater than 0.05, it was considered insignificant.

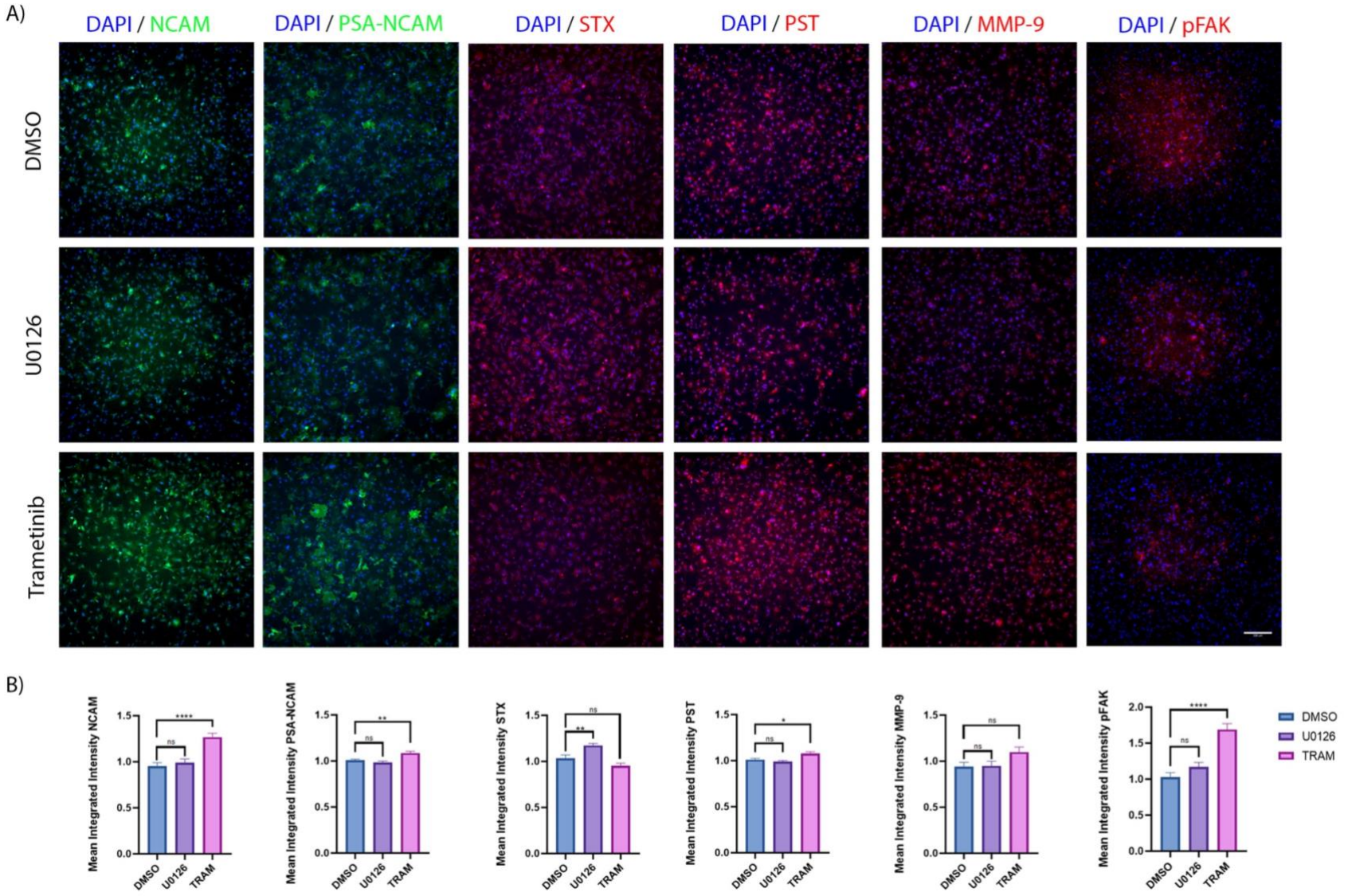

Figure 5. The effects of MEK inhibitors on various migratory markers in patient-derived T115 GBM case exhibited two-dimensional cell morphology.

T115 GBM cells were incubated with 100 nM trametinib or 1 μM U0126 or control (0.01% DMSO) for 48 hours. (A) Representative images of NCAM, PSA-NCAM, STX, PST, MMP-9 and phosphorylated FAK signalling in the presence of either MEK inhibitor and control (DMSO) in T115.19 repeat. (B) The mean cytoplasmic integrated intensity of NCAM, PSA-NCAM, STX, PST, MMP-9 and phosphorylated FAK was normalised to control (0.01% DMSO). ns = not significant where $p > 0.05$, * $p < 0.05$, ** $p < 0.01$, *** $p < 0.001$, **** $p < 0.0001$ significance relative to control (DMSO) via one-way ANOVA and Dunnet post-hoc test. $n = 3$ repeats of T115, scale bar = 200 μm.

After the initial high-throughput characterisation of migratory markers in GBM via ICC monolayered cells, the same markers were further investigated in three-dimensional tumour cell morphology using tumour spheroids because monolayered cells fail to represent tumour cell morphology within patients accurately. The purpose of this experimentation was to examine any potential differences in two-dimensional and three-dimensional tumour cell morphology as tumour cells express various growth factors to retain their spherical shape as well as interact with the surrounding environment for attachment, migration, and invasion (Friedl & Wolf, 2003; Gensbittel et al., 2021; Hanahan & Weinberg, 2011a; Suresh, 2007; Zhou et al., 2015).

Following the acquisition of tumour spheroid images, the individual images were montaged using MetaXpress® software into a larger image due to the imaging limitation of the ImageXpress® Micro XLS system. The tumour spheroid analysis begins with masking the core of the tumour sphere as the focus of this experimentation was to investigate the overall difference in signalling intensity of various markers within tumour cells migrating from the tumour core when treated with MEK inhibitors. An automated boundary was set around the core and omitted, leaving behind the outer region that consisted of individual tumour cells that had migrated from the tumour core. Following this, an automated threshold was set to analyse the signalling intensity of each marker via ZEN microscopy software. The automated threshold excluded dark cells (no signal) and cells with insufficient signalling difference between the marker of interest and the background. The analysis resulted in the area of individual tumour cells that had migrated from the core expressing the marker of interest and the intensity of each individual cell expressing the marker of interest.

The data obtained from ICC tumour spheroid analysis was converted from pixel^2 to square micrometers (μm^2) by the division of 9.614806802 in Excel before statistical analysis was conducted in Prism. Within each repeat, two tumour spheres were allocated to each condition (control, 0.01% DMSO, U0126, and trametinib). Data presented in figure 6 has been normalised to the average relative control, 0.01% DMSO before a one-way ANOVA and Dunnet post-hoc test was performed on the two repeats of T115 GBM tumour spheres (n = 2).

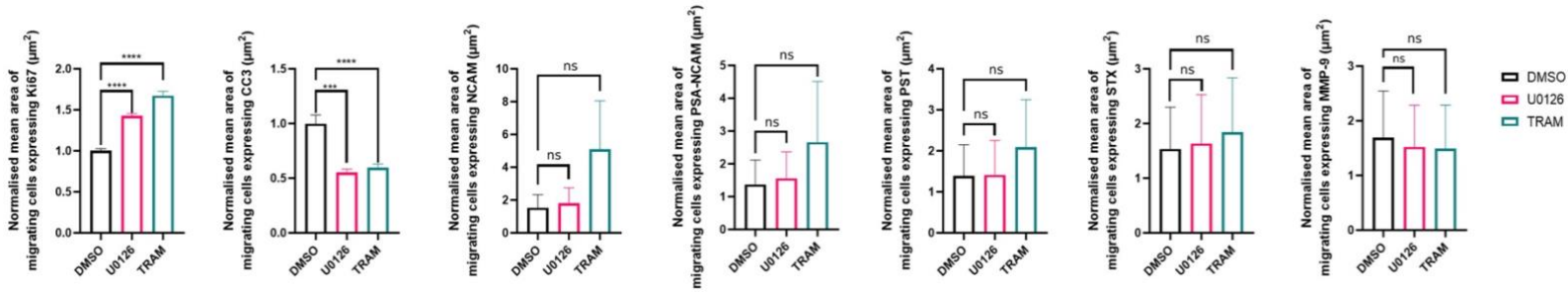

Figure 6. The effects of MEK inhibitors on various migratory markers in patient-derived T115 GBM case exhibited three-dimensional cell morphology.

T115 GBM cells were incubated with 100 nM trametinib or 1 μM U0126 or control (0.01% DMSO) for 48 hours. The mean area of migrating cells expressing either the proliferative (Ki67), apoptotic cell death (CC3) or majority markers (NCAM, PSA-NCAM, STX, PST and MMP-9) was normalised to the average value of control (0.01% DMSO) and presented as μm^2. ns = not significant where $p > 0.05$, * $p < 0.05$, ** $p < 0.01$, *** $p < 0.001$, **** $p < 0.0001$ significance relative to control (DMSO) via one-way ANOVA and Dunnet post-hoc test. $n = 2$ repeats of T115, scale bar = 200 μm.

Following the exploration of migratory markers in two-dimensional cell morphology, the same markers were investigated in three-dimensional cell morphology. The data shown in figure 6 only show a significant difference between the three treatment conditions in the proliferative and apoptotic cell death markers. Interestingly in the presence of trametinib and U0126, cells migrating from the core had greater expression of Ki67 compared to the control ($p < 0.0001$). On the other hand, CC3 expression significantly decreased in cells migrating from the core when treated with either MEK inhibitor in contrast to the control ($p < 0.0001$ for trametinib and $p < 0.001$ for U0126).

Both NCAM and PSA-NCAM appear to be greatly increased in migrating cells treated with trametinib compared to control. In those migrating cells treated with U0126, a slight increase in NCAM and PSA-NCAM was seen (figure 6). However, these findings are not statistically significant. Additionally, the two enzymes of PSA-NCAM, STX and PST, also demonstrated a slight increase in those cells treated with trametinib and U0126 compared to the control. In contrast to the control, migrating cells elicited a slightly reduced expression of MMP-9 in both trametinib and U0126 conditions. Nevertheless, these findings were also statistically insignificant.

Unfortunately, there is no significant difference in any of the migratory markers when treated with MEK inhibitors. The comparison between two-dimensional and three-dimensional migratory marker signalling in the presence of MEK inhibitors is reviewed in the discussion.

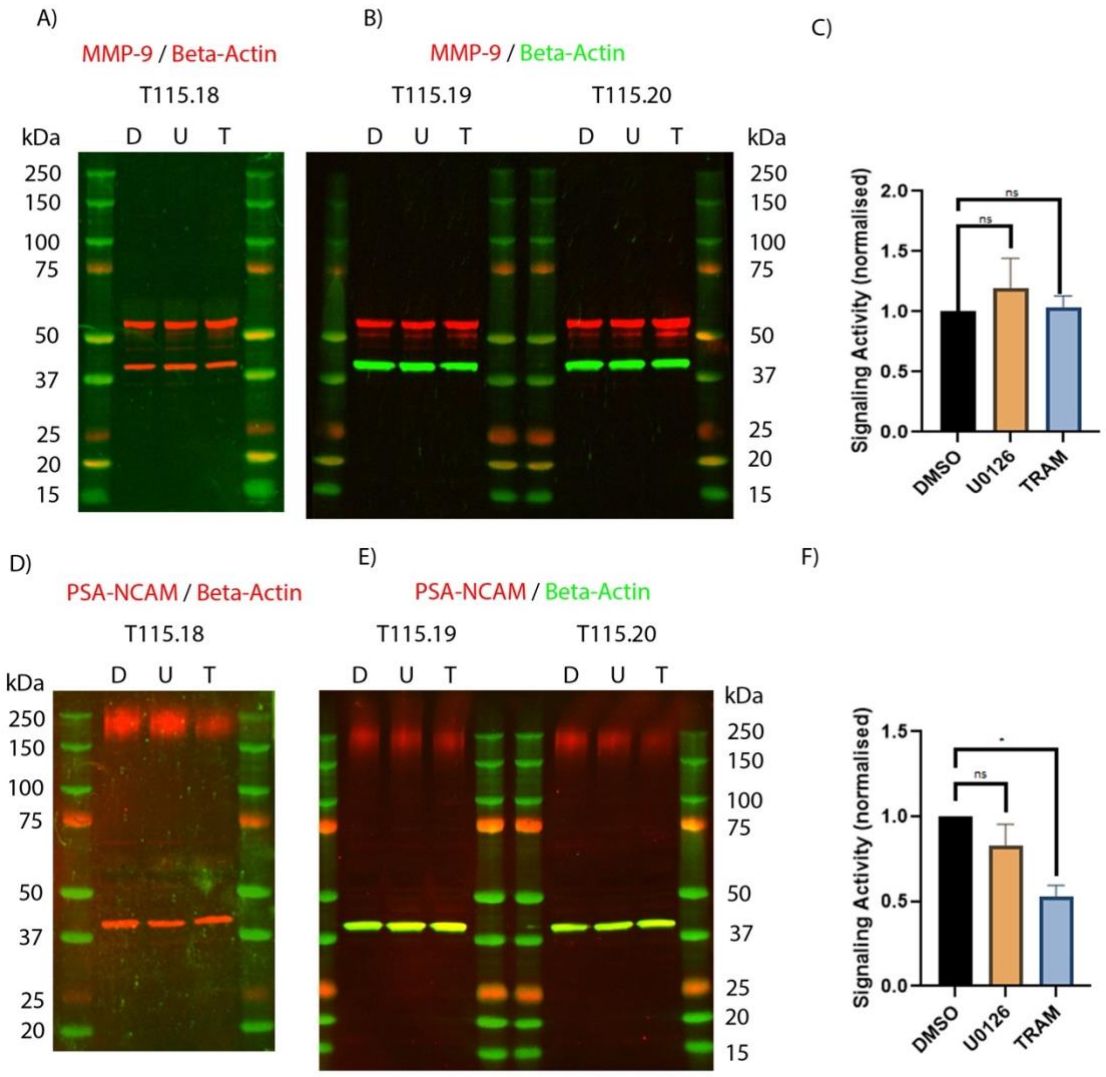

Figure 7. Trametinib inhibits PSA-NCAM protein expression in T115 patient-derived GBM tumourspheres.

T115 GBM tumourspheres were treated with 100 nM trametinib or 1 μM U0126 or control (0.01% DMSO) for 48 hours to investigate changes in protein expression due to MEK inhibitors. (A-B) Western blot images of three repeats of T115 stained for MMP-9 (red) and β-actin (green/red). (A) Blot was stripped and restained with β-actin (red) after initial staining with MMP-9 (red) and L1CAM (not present). (D-E) Western blot images of three repeats of T115 stained for PSA-NCAM (red) and β-actin (green/red). (D) Similar to (A), blot was stripped and restained with β-actin (red) after initial staining with PSA-NCAM (red) and NCAM (not present). (C,F) ns = not significant, * $p < 0.05$, ** $p < 0.01$, *** $p < 0.001$, **** $p < 0.0001$ significance relative to control (DMSO) via one-way ANOVA and Dunnet post-hoc test. $n = 3$ repeats of T115**.**

Following the mass screening of migratory, proliferative, apoptotic, and cell cycle-associated genes, and the characterisation of migratory markers via ICC, specific migratory markers were chosen for western blot validation. One of the markers was MMP-9, as a strong down-regulated of the MMP-9 gene was found in my results. In addition, researchers have shown MMP-9 to have associations with MEK pathways specifically (J. Gao et al., 2019; Guo et al., 2020; Simon et al., 1999). Another marker that was further validated was PSA-NCAM, as the initial PCR screening demonstrated a strong upregulation in the NCAM gene. Furthermore, PSA is a post-translational modification of NCAM (Cremer et al., 2000).

U0126, trametinib, and control conditions had 30 μg of protein per μL loaded in each lane across three repeats of T115 GBM tumourspheres. Each blot was stained with one primary marker and β – actin which served as the housekeeping gene. Blots were stripped in methanol for restaining with a new marker. Unfortunately, the NCAM stain did not appear on the blot but, PSA-NCAM and MMP-9 did. Blots were plotted as mean +/- SEM and normalised to the intensity of its respective β-actin housing acting gene before being normalised to its respective control (0.01% DMSO) and statistically analysed via a one-way ANOVA and Dunnet's post hoc test.

Based on the PCR screening (figure 4), MMP-9 was strongly downregulated when treated with trametinib. However, no significant difference was observed when MMP-9 protein expression across the three conditions was explored (figure 7, A-C). This was consistently seen across the three repeats of T115 tumourspheres. On the other hand, a significant difference was observed when PSA-NCAM protein expression was investigated in terms of trametinib-treated cells compared to the control (0.01% DMSO) (figure 7, F). This significant difference was seen across the three conditions in all three repeats of T115 tumourspheres and correlates with the strong upregulation in the NCAM gene seen in the qRT-PCR screen. Unfortunately, there is no significant difference in PSA-NCAM protein expression in the U0126 treated cell compared to the control (0.01% DMSO) (figure 7, F).

3.4. Exploring cell migration patterns in MEK inhibitor-treated tumourspheres over 96 hours

Tumour cells exist in a three-dimensional morphology and attach as well as interact with brain tissue for migration and invasion (Curtin et al., 2021). To account for this, live-cell migration experiments were conducted with T115 spheroids grown in a free-floating plate that stimulated spheroid formation (as mentioned in subsection 1.2.3). The spheres were transferred into 24-well plates for roughly 2-3 hours before the addition of their respective MEK inhibitors. The live cell migration experiment was conducted for 96 hours. However, the analysis is limited to roughly 18 hours because the imaging field is limiting and tumour cells migrate out of the imaging frame after 24 hours. It became impossible to track or quantify tumour cells. The live cell experiments were conducted on one patient-derived GBM cases, T115, and repeated thrice (n = 3).

Live cell migration experiments demonstrate the real-time effects of the MEK inhibitors on T115 tumourspheres over a 96-hour duration. The live cell analysis enabled visualisation and quantification of tumoursphere migration across the three conditions. The migration rate was determined by measuring the deformation of migrating areas of the tumourspheres at various time points. The velocity and distance travelled by individual cells can also be determined. The migration rate for each tumoursphere was calculated via the outermost migrating cells as they were the most representative (detailed in (Vong et al., 2022). The quantification is limited by the outermost migratory cells (discussed further in chapter 4). The top of figure 11 illustrates each repeat of the live cell experiment on T115 tumourspheres. The bottom graph is the combined results of all three repeats. Statistically significant relative to its control (0.01% DMSO) was conducted via a two-way ANOVA and Tukey' post hoc test.

Figures 8-10 demonstrate overall tumour spheroid cell migration in the first 24 hours of treatment with either MEK inhibitor or 0.01% DMSO (control). Trametinib treatment resulted in an overall reduction in sphere size and consistently seen in all three repeats. Moreover, the treatment of U0126 resulted in similar migration pattern as our control, DMSO. At the 24th hour across all three repeats, it is extremely apparent that trametinib is the more effective inhibitor of tumour cell migration in contrast to U0126 and control (0.01% DMSO) (figure 8-10). From the live cell analysis, there is a significant reduction in the percentage of the overall rate of migration of tumour spheres treated with trametinib (normalised to its respective control, 0.01% DMSO) (figure 11). From the eighth hour of the

live cell experiment to the eighteenth hour, tumourspheres treated with trametinib demonstrated a statistical significance ranging between $p < 0.05$ and $p < 0.01$ (figure 11). On the other hand, U0126 exhibited statistical significance only at the sixteenth hour of live cell experiments.

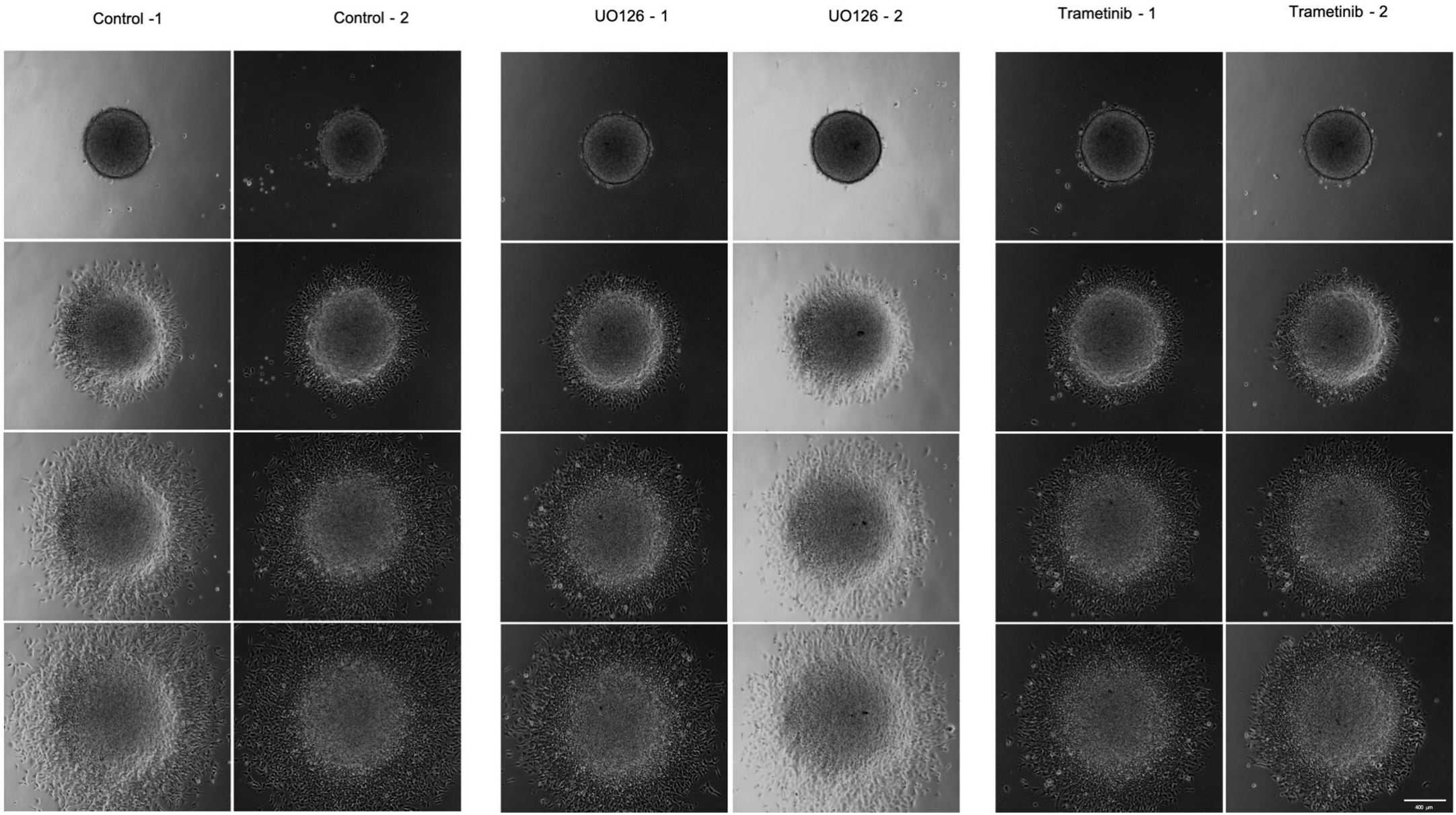

Figure 8. T115.18 patient-derived GBM tumourspheres at 0 hour, 8 hour, 16 hour and 24 hour points during the 96-hour live cell migration experiment. Scale bar: 400 µm

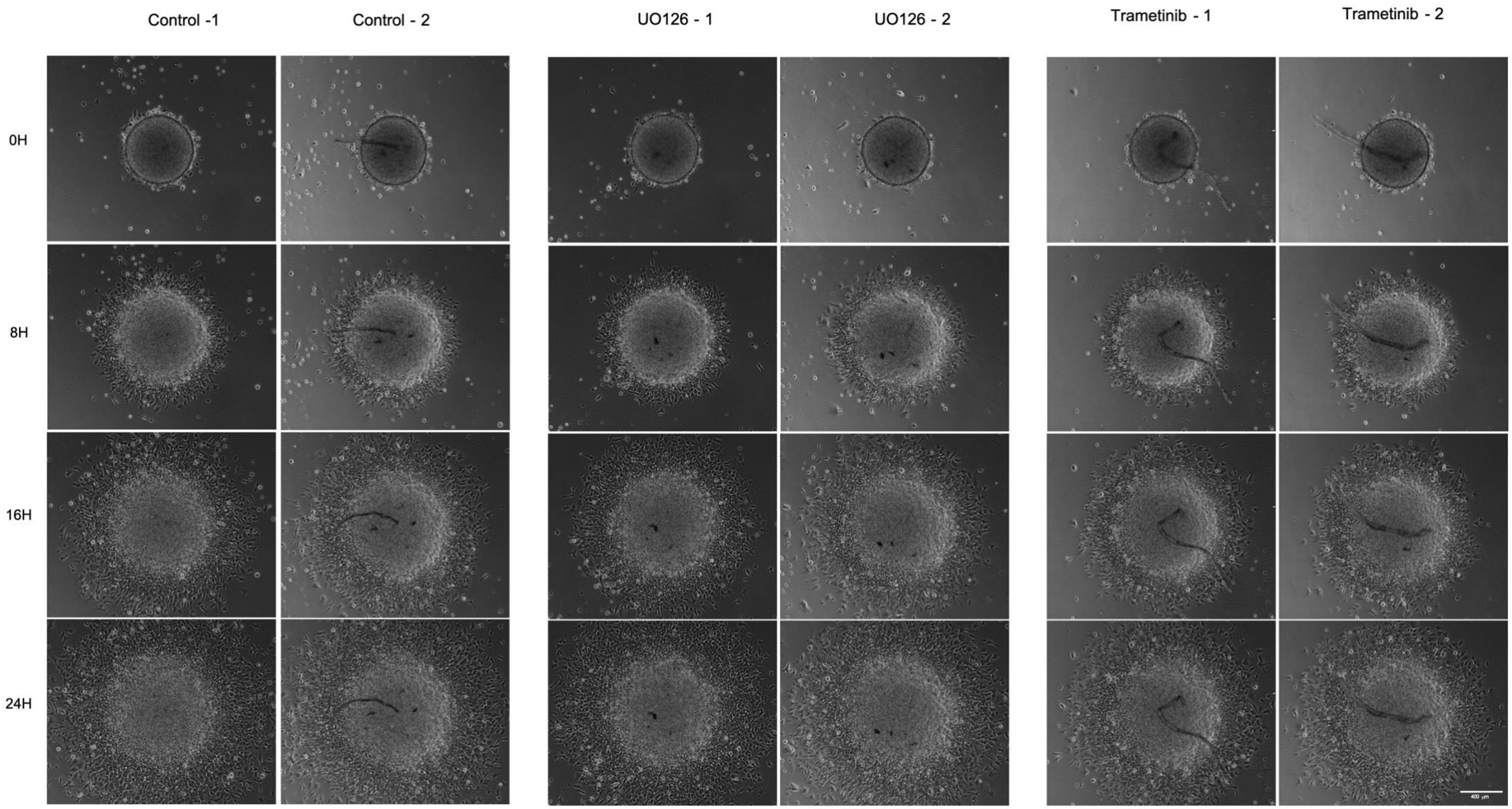

Figure 9. T115.19 patient-derived GBM tumourspheres at 0 hour, 8 hour, 16 hour and 24 hour points during the 96-hour live cell migration experiment. Scale bar: 400 µm

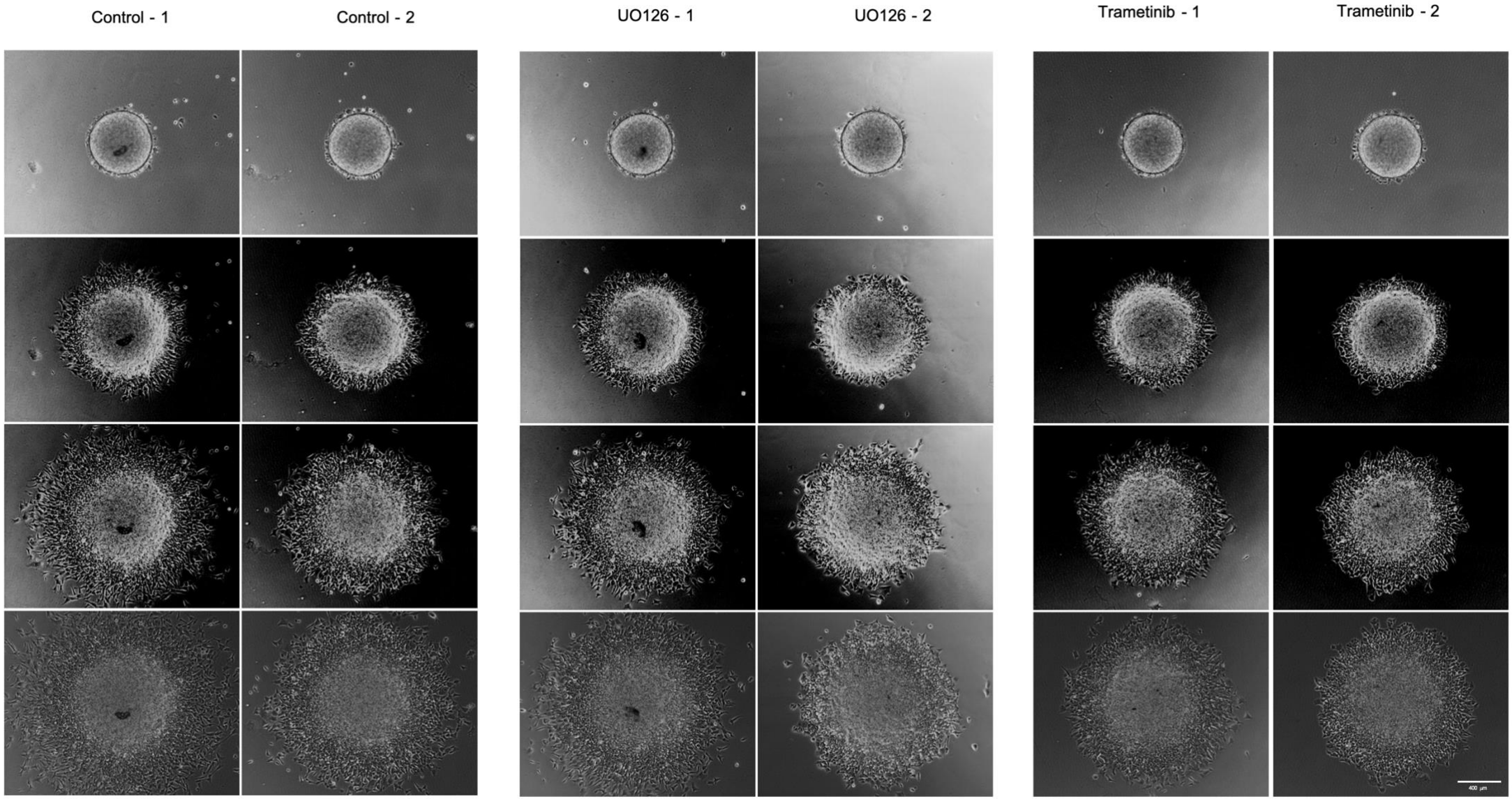

Figure 10. T115.20 patient-derived GBM tumourspheres at 0 hour, 8 hour, 16 hour and 24 hour points during the 96-hour live cell migration experiment. Scale bar: 400 µm

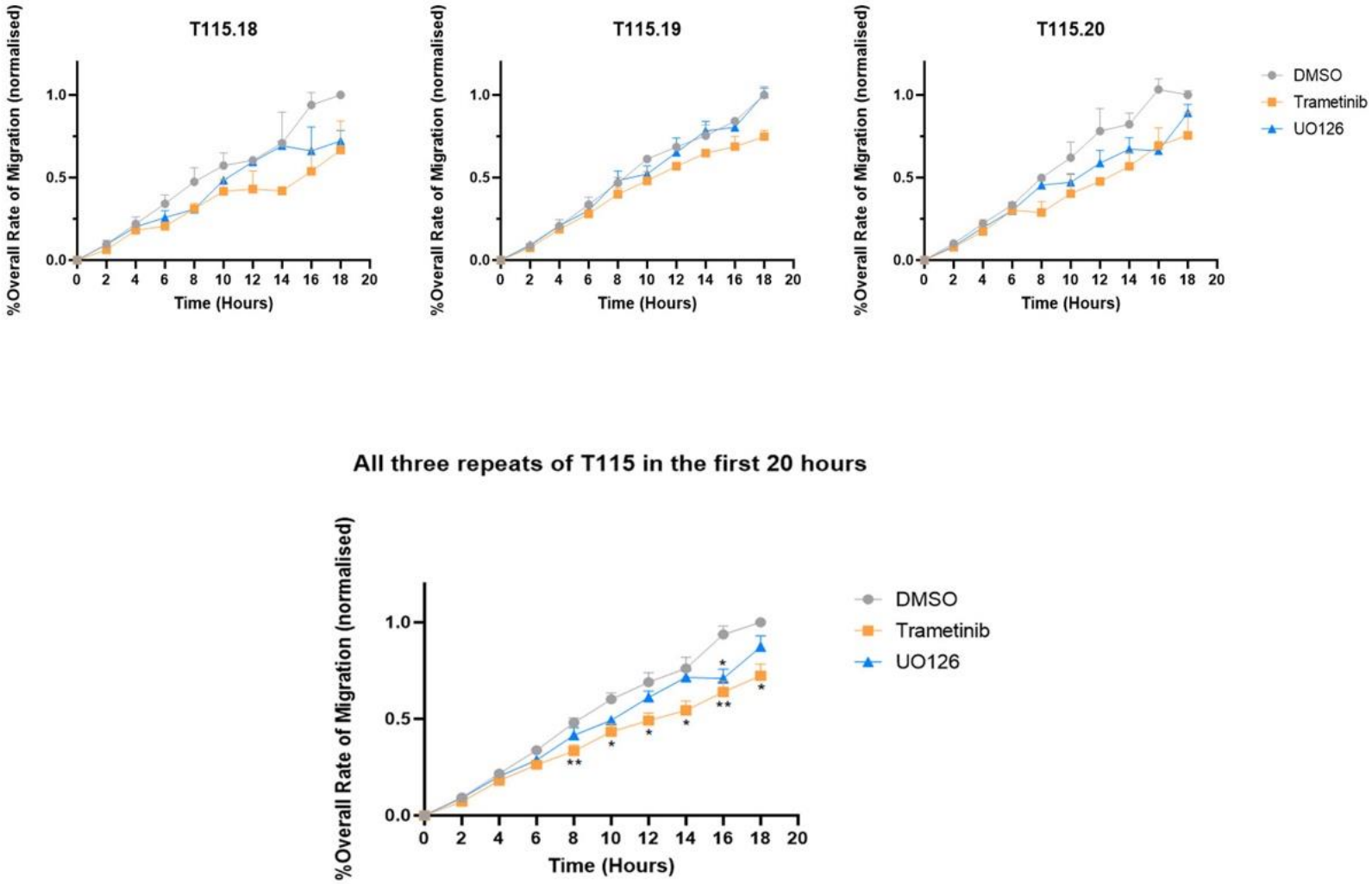

Figure 11. Live Cell Migration Analysis across all three repeats of T115.

Two tumourspheres were treated with each condition (trametinib, U0126 and the control 0.01% DMSO), forming one repeat. The live cell migration experiment was conducted for 96 hours, however due to the limitation of the imaging frame the analysis is limited to roughly the first 24 hours. * $p < 0.05$, ** $p < 0.01$, *** $p < 0.001$, **** $p < 0.0001$ significance relative to control (DMSO) via two-way ANOVA and Tukey's post-hoc test. Live cell migration analysis was conducted by Chun Kiet Vong. n = 3 repeats of T115.

Chapter 4. Discussion

4.1. Overall findings

There is an urgent need for the development of effective therapeutics against GBM, with the last global advancement (Stupp's protocol) occurring nearly 20 years ago (Stupp et al., 2005). This thesis investigated the potential benefits of utilising MEK inhibitors in the treatment of GBM, focusing on the limitation of GBM tumour cell migration.

In the past, researchers have attempted to target various points along the MAPK signalling cascade but faced many difficulties as the pathway is critical in relaying signals and has numerous crosstalk and interaction points (Braicu et al., 2019; Chappell et al., 2011; Y. Sun et al., 2015). The implications of the MEK/ERK portion of the MAPK cascade have also been explored with respect to GBM migration and tumorigenicity (Sunayama et al., 2010). The migratory markers chosen in this thesis have also been connected with the MEK/ERK pathway. For instance, PSA-NCAM is considered as an adverse prognostic marker of GBM (M. C. Amoureux et al., 2010; Seidenfaden et al., 2003) as the attachment of polySia disrupts the interactions between NCAM and other cells. It is also speculated to contribute to GBM migration and invasion (Suzuki et al., 2005). Furthermore, MMP-9 is implicated in the migration and invasive capabilities of GBM, and the MEK/ERK pathways are involved in regulating MMP-9 signalling (Lakka et al., 2002). However, a direct relation between the chosen migratory markers and the MEK/ERK pathway remains to be established.

Trametinib and U0126 suppress the phosphorylation abilities of MEK-1 and MEK-2 and cause a reduction in downstream ERK1/2 signalling (McLendon et al., 2008). Overall, our findings have showcased that trametinib is a more effective inhibitor of MEK-1 and MEK-2 when compared to U0126 and the control DMSO. In 2007, trametinib was discovered to be highly specific towards MEK1/2 (determined via a protein kinase array experiment) (Yamaguchi & Condeelis, 2007) and explains potentially why trametinib is more effective than U0126.

For the most part, U0126 was demonstrated as a less effective inhibitor of MEK-1 and MEK-2 subsets compared to the control, DMSO, and trametinib. A possible reason for this could be due to the drug design and binding affinity of U0126 (Duncia et al., 1998; English & Cobb,

2002). Dunica et al., (1998) discovered that U0126 exhibited non-competitive inhibition of MEK-1 and MEK-2 with an IC_{50} of 0.07 μM for MEK-1 and 0.06 μM for MEK-2. The drug can also undergo isomerisation *in vivo* and exhibits less affinity for MEK (Duncia et al., 1998). Some studies have found that U0126 also inhibits the kinase activity of MEK5 at concentrations above 3 μM, therefore, attenuating ERK5 phosphorylation downstream, in addition to preventing MEK-1 and MEK-2 kinase activity (Davies et al., 2000; Mody et al., 2001). MEK-5 signalling cascade is distinct from MEK-1 and MEK-2 signalling (English & Cobb, 2002; X. Wang & Tournier, 2006). However, as we used 1 μM of U0126 consistently throughout all the experiments, it is more likely that U0126 was a less effective inhibitor as the drug noncompetitively inhibits MEK-1 and MEK-2 and possibly undergone isomerisation within the tumour cells (Duncia et al., 1998; English & Cobb, 2002).

The comparison between two-dimensional and three-dimensional migratory marker signalling in patient-derived tumour cells in the presence of MEK inhibitors did not yield statistically significant results. However, some estimated trends did emerge from comparing the two cell models. The treatment of trametinib increases NCAM and PSA-NCAM expression in both monolayered and spheroid cells when compared to control.

Another marker displaying a similar trend is PST as in the monolayered cells and in the cells migrating from the tumour sphere core expressed an increase in signalling when treated with trametinib in contrast to control. However, in both monolayered and spheroid cells that were treated with U0126, the expression of PST was similar to control.

Interestingly, the STX signal when treated with trametinib in monolayered cells decreased while it increased in spheroid cells (compared to control). U0126 treated monolayer cells exhibited a significant increase in STX (compared to control), whereas spheroid cells exhibited a similar trend as the control but were considered not significant.

An opposing trend was also seen in MMP-9 signalling when treated with trametinib. In the monolayered cells, MMP-9 signalling increased slightly compared to control, while in the spheroid cells, a slight decrease was seen (in contrast to control). Similarly, when treated with U0126, monolayered cells expressed a signalling response similar to control. But, in spheroid cells, a slight decrease in MMP-9 was exhibited.

The use of tumour spheroids provided a better representation of tumour cell biology because it better reflected the three-dimensional tissues and cellular aspects of GBM in contrast to

conventional migration analysis, which uses monolayered tumour cells that are adherent to the base of the well (Gudbergsson et al., 2019; Kang et al., 2015).

As mentioned above, there were variable migratory marker signalling responses in the presence of either MEK inhibitor. For instance, MMP-9 is shown to be down-regulated when ERK1/2 phosphorylation is altered (Dontula et al., 2013). In addition, Arai et al., (2003) found that inhibition of the ERK pathway via U0126 significantly reduced MMP-9 upregulation (Arai et al., 2003). However, this was not seen in our findings as MMP-9 did not appear to follow a consistent trend when treated with either trametinib and U0126. It is highly possible that the lack of a representative tumour microenvironment resulted in our inconsistent findings as MMP-9 directly degrades the ECM (Lakka et al., 2002).

Two migratory markers that displayed consistent trends in the presence of MEK inhibitors were NCAM and PSA-NCAM. However, the increase in NCAM and PSA-NCAM signalling produces confusion as NCAM functions as a cell adhesion molecule while PSA-NCAM disrupts the cell adhesion function of NCAM, enabling the cell to migrate (Cremer et al., 2000; Ditlevsen et al., 2008; Muller et al., 1996). It is possible that the increase in PSA-NCAM signalling observed is due to the subpopulation of GSCs, as these cells possess stem-like qualities and are considered resistant to radiation and chemotherapy (Cheng et al., 2010; Sanai et al., 2005; Zepecki et al., 2019). On the other hand, an increase in NCAM signalling resulted in the reduction of tumour cell migration as the tumour suppressive quality of NCAM was initiated in the presence of the MEK inhibitors (Sasaki et al., 1998; Seifert et al., 2012). Furthermore, in neurons, NCAM signalling occurs via FAK and MEK to induce CREB (a cellular transcription factor). Therefore, inhibiting MEK could result in compensatory upregulation of NCAM (Hinkle et al., 2006; Kolkova et al., 1994) and may explain the increase in NCAM signalling in our results.

Aforementioned, the changes in the genetic expression of markers explored via qRT-PCR did not necessarily lead to changes in protein expression as seen by the western validation data. This could be explained by the delay between transcription (mRNA) and translation (protein). The delayed synthesis occurs as maturation, exportation, and translation of mRNA require time. It is possible that the time point chosen for protein validation in this thesis failed to capture the delayed synthesis (Y. Liu et al., 2016). Future studies should consider exploring various timepoints for protein validation and qRT-PCR to reflect better tumour biological changes occurring in the presence of MEK inhibitors.

Most of this study was conducted on one patient-derived T115 GBM case and lacked consideration of the heterogeneity present within GBM cases. However, as there are three repeats for nearly all experiments, the methodologies used in this thesis can be considered robust, and the findings from this thesis can be utilised to form the basis of future studies exploring the use of MEK inhibitors to modulate migration.

The lack of proliferation control may be a minor limitation of this thesis. Previously, a mitotic inhibitor cocktail, AraC/2dCTD, was used to control for proliferation within experiments that explored the effects of MEK inhibitors on migration in our lab since AraC/2dCTD did not influence the MEK/ERK pathway (Christman, 2002). But, it is difficult to control for proliferation as without this process, cells cannot grow and migrate (Kim, 2013). In addition, the two are often explored together in the field, and therefore, the need to control for proliferation in any of the experiments was not deemed necessary. In addition, the proliferation activity (determined by the EdU assay) between U0126 and trametinib were roughly similar, but trametinib resulted in greater attenuation of the migration. Furthermore, U0126 exhibited lower proliferation compared to the control (0.01% DMSO). In addition, in our live cell migration findings, U0126 exhibited similar overall tumour cell migration as control (0.01% DMSO) (figure 8-10). We can conclude that proliferation does not heavily contribute to the migration of tumour cells. An additional improvement to the migration assay could include tracking individual cells in addition to the overall migration area. This will allow finer quantification of the drug's effect on cell migration, such as cellular velocity.

In summation, this study aimed to investigate the effects of MEK inhibitors on GBM tumour cell migration and achieved this in at least one patient-derived GBM case. Based on my results, there is potential for trametinib to be an effective inhibitor of tumour cell migration via modulation of the MEK/ERK pathway. But, more repeats in different GBM cases are required to confidently state that trametinib is an effective inhibitor of GBM tumour migration. The comparison of migratory marker expression in two-dimensional cell morphology and three-dimensional cell morphology (tumourspheres) was also investigated in this thesis. Compared to conventional monolayer migration assays, the use of tumourspheres to investigate the effect of MEK inhibitors on tumour cell migration did not yield significant results as we expected. This may be due to the lack of consideration for a representative surrounding environment in which the tumour spheres can be investigated in, despite having representative tumour biology. Specifically, three-dimensional spheres were plated onto a flat two-dimensional surface. The complex nature of GBM requires a multifaceted approach that

considers not only tumour cell biology but also the surrounding tumour environment. Future studies exploring the three-dimensional tumour microenvironment may result in findings that have never been explored in GBM literature. This could be conducted by producing a Matrigel-coated well that mimics the surface of the brain as well as grooves and ridges so that the tumoursphere cells can migrate through the gel, and we can observe the modulation of the tumour microenvironment as well as tumour biology that enables tumour cells to migrate and invade the surrounding healthy brain tissue. All-in-all, this thesis has highlighted the potential for MEK inhibitors to modulate GBM cell migration through a model that is closely representative of the tumour morphology and biology within patients.

References

Ahluwalia, M. S., Groot, J. de, Liu, W. M., & Gladson, C. L. (2010). Targeting SRC in glioblastoma tumors and brain metastases: Rationale and preclinical studies. In *Cancer Letters* (Vol. 298, Issue 2, pp. 139–149). Elsevier Ireland Ltd. https://doi.org/10.1016/j.canlet.2010.08.014

Alessi, D. R., Saito, Y., Campbell, D. G., Cohen, P., Sithanandam, G., Rapp, U., Ashworth, A., Marshall, C. J., & Cowley, S. (1994). Identification of the sites in MAP kinase kinase-1 phosphorylated by p74(raf-1). *EMBO Journal*, *13*(7), 1610–1619. https://doi.org/10.1002/j.1460-2075.1994.tb06424.x

Al-Saraireh, Y. M. J., Sutherland, M., Springett, B. R., Freiberger, F., Ribeiro Morais, G., Loadman, P. M., Errington, R. J., Smith, P. J., Fukuda, M., Gerardy-Schahn, R., Patterson, L. H., Shnyder, S. D., & Falconer, R. A. (2013). Pharmacological Inhibition of polysialyltransferase ST8SiaII Modulates Tumour Cell Migration. *PLoS ONE*, *8*(8). https://doi.org/10.1371/journal.pone.0073366

Amoureux, M. C., Coulibaly, B., Chinot, O., Loundou, A., Metellus, P., Rougon, G., & Figarella-Branger, D. (2010). Polysialic acid neural cell adhesion molecule (psa-ncam) is an adverse prognosis factor in glioblastoma, and regulates olig2 expression in glioma cell lines. *BMC Cancer*, *10*. https://doi.org/10.1186/1471-2407-10-91

Amoureux, M.-C., Coulibaly, B., Chinot, O., Loundou, A., Metellus, P., Rougon, G., & Figarella-Branger, D. (2010). Polysialic Acid Neural Cell Adhesion Molecule (PSA-NCAM) is an adverse prognosis factor in glioblastoma, and regulates olig2 expression in glioma cell lines. In *BMC Cancer* (Vol. 10). http://www.biomedcentral.com/1471-2407/10/91

Arai, K., Lee, S. R., & Lo, E. H. (2003). Essential role for ERK mitogen-activated protein kinase in matrix metalloproteinase-9 regulation in rat cortical astrocytes. *GLIA*, *43*(3), 254–264. https://doi.org/10.1002/glia.10255

Bànkfalvi, A., Piffkò, J., & Gnes Bánkfalvi, A. `. (2000). Prognostic and predictive factors in oral cancer: the role of the invasive tumour front. *J Oral Pathol Med. J Oral Pathol Med*, *29*, 291–299.

Bao, S., Wu, Q., McLendon, R. E., Hao, Y., Shi, Q., Hjelmeland, A. B., Dewhirst, M. W., Bigner, D. D., & Rich, J. N. (2006). Glioma stem cells promote radioresistance by preferential activation of the DNA damage response. *Nature*, *444*(7120), 756–760. https://doi.org/10.1038/nature05236

Baskar, R., Lee, K. A., Yeo, R., & Yeoh, K. W. (2012). Cancer and radiation therapy: Current advances and future directions. In *International Journal of Medical Sciences* (Vol. 9, Issue 3, pp. 193–199). https://doi.org/10.7150/ijms.3635

Battista, D., & Rutishauser, U. (2010). Removal of polysialic acid triggers dispersion of subventricularly derived neuroblasts into surrounding CNS tissues. *Journal of Neuroscience*, *30*(11), 3995–4003. https://doi.org/10.1523/JNEUROSCI.4382-09.2010

Begg, A. C., Stewart, F. A., & Vens, C. (2011). Strategies to improve radiotherapy with targeted drugs. In *Nature Reviews Cancer* (Vol. 11, Issue 4, pp. 239–253). https://doi.org/10.1038/nrc3007

Biserova, K., Jakovlevs, A., Uljanovs, R., & Strumfa, I. (2021). Cancer Stem Cells: Significance in Origin, Pathogenesis and Treatment of Glioblastoma. In *Cells* (Vol. 10, Issue 3). NLM (Medline). https://doi.org/10.3390/cells10030621

Braicu, C., Buse, M., Busuioc, C., Drula, R., Gulei, D., Raduly, L., Rusu, A., Irimie, A., Atanasov, A. G., Slaby, O., Ionescu, C., & Berindan-Neagoe, I. (2019). A comprehensive review on MAPK: A promising therapeutic target in cancer. In *Cancers* (Vol. 11, Issue 10). MDPI AG. https://doi.org/10.3390/cancers11101618

Brat, D. J., & The Cancer Genome Atlas Research Network. (2015). Comprehensive, Integrative Genomic Analysis of Diffuse Lower-Grade Gliomas. *New England Journal of Medicine*, *372*(26), 2481–2498. https://doi.org/10.1056/NEJMoa1402121

Btirk, R. R. (1973). A Factor from a Transformed Cell Line That Affects Cell Migration. *Proceedings of the National Academy of Sciences of the United States of America*, *70*(2), 369–372. https://www.pnas.org

Butowski, N. A. (2015). Epidemiology and Diagnosis of Brain Tumors. *American Academy of Neurology*, *21*(2), 301–313. www.ContinuumJournal.com

Carruthers, R., Ahmed, S. U., Strathdee, K., Gomez-Roman, N., Amoah-Buahin, E., Watts, C., & Chalmers, A. J. (2015). Abrogation of radioresistance in glioblastoma stem-like cells by inhibition of ATM kinase. *Molecular Oncology*, *9*(1), 192–203. https://doi.org/10.1016/j.molonc.2014.08.003

Cayre, M., Canoll, P., & Goldman, J. E. (2009). Cell migration in the normal and pathological postnatal mammalian brain. In *Progress in Neurobiology* (Vol. 88, Issue 1, pp. 41–63). https://doi.org/10.1016/j.pneurobio.2009.02.001

Chang, F., Steelman, L. S., Lee, J. T., Shelton, J. G., Navolanic, P. M., Blalock, W. L., Franklin, R. A., & McCubrey, J. A. (2003). Signal transduction mediated by the Ras/Raf/MEK/ERK pathway from cytokine receptors to transcription factors: Potential targeting for therapeutic intervention. In *Leukemia* (Vol. 17, Issue 7, pp. 1263–1293). Nature Publishing Group. https://doi.org/10.1038/sj.leu.2402945

Chappell, W. H., Steelman, L. S., Long, J. M., Kempf, R. C., Abrams, S. L., Franklin, R. A., Bäsecke, J., Stivala, F., Donia, M., Fagone, P., Malaponte, G., Mazzarino, M. C., Nicoletti, F., Libra, M., Maksimovic-Ivanic, D., Mijatovic, S., Montalto, G., Cervello, M., Laidler, P., … Mccubrey, J. A. (2011). Ras/Raf/MEK/ERK and PI3K/PTEN/Akt/mTOR Inhibitors: Rationale and Importance to Inhibiting These Pathways in Human Health. In *Oncotarget* (Vol. 2, Issue 3). www.impactjournals.com/oncotarget/www.impactjournals.com/oncotargetwww.impactjournals.com/oncotarget

Chen, Y., & Xu, R. (2016). Drug repurposing for glioblastoma based on molecular subtypes. *Journal of Biomedical Informatics*, *64*, 131–138. https://doi.org/10.1016/j.jbi.2016.09.019

Cheng, L., Bao, S., & Rich, J. N. (2010). Potential therapeutic implications of cancer stem cells in glioblastoma. In *Biochemical Pharmacology* (Vol. 80, Issue 5, pp. 654–665). https://doi.org/10.1016/j.bcp.2010.04.035

Cheung, K. J., & Ewald, A. J. (2014). Illuminating breast cancer invasion: Diverse roles for cell-cell interactions. In *Current Opinion in Cell Biology* (Vol. 30, Issue 1, pp. 99–111). Elsevier Ltd. https://doi.org/10.1016/j.ceb.2014.07.003

Christman, J. K. (2002). 5-Azacytidine and 5-aza-2'-deoxycytidine as inhibitors of DNA methylation: mechanistic studies and their implications for cancer therapy. *Oncogene*, *21*, 5483–5495. https://doi.org/10.1038/sj.onc

Cremer, H., Chazal, G., Lledo, P. M., Rougon, G., Montaron, M. F., Mayo, W., le Moal, M., & Abrous, D. N. (2000). PSA-NCAM: An important regulator of hippocampal plasticity. *International Journal of Developmental Neuroscience*, *18*(2–3), 213–220. https://doi.org/10.1016/S0736-5748(99)00090-8

Cremer, H., Lange, R., Christoph, A., Plomann, M., Vopper, G., Roes, J., Brown, R., Baldwin, S., Kraemer, P., Scheff, S., Barthels, D., Rajewksy, K., & Wille, W. (1994). Inactivation of theN-CAM gene in mice results in size reduction of the olfactory bulb and deficits in spatial learning. *Nature*, *367*, 455–459.

Crespo, I., Vital, A. L., Nieto, A. B., Rebelo, O., Tão, H., Lopes, M. C., Oliveira, C. R., French, P. J., Orfao, A., & Tabernero, M. D. (2011). Detailed characterization of alterations of chromosomes 7, 9, and 10 in glioblastomas as assessed by single-nucleotide polymorphism arrays. *Journal of Molecular Diagnostics*, *13*(6), 634–647. https://doi.org/10.1016/j.jmoldx.2011.06.003

Crossin, K. L., & Krushel, L. A. (2000). Cellular Signaling by Neural Cell Adhesion Molecules of the Immunoglobulin Superfamily. *Developmental Dynamics*, *218*, 260–279.

Curtin, L., Whitmire, P., White, H., Bond, K. M., Mrugala, M. M., Hu, L. S., & Swanson, K. R. (2021). Shape matters: morphological metrics of glioblastoma imaging abnormalities as biomarkers of prognosis. *Scientific Reports*, *11*(1). https://doi.org/10.1038/s41598-021-02495-6

Curtis, M. A., Kam, M., Nannmark, U., Anderson, M. F., Axell, M. Z., Wikkelso, C., Holtås, S., van Roon-Mom, W. M. C., Björk-Eriksson, T., Nordborg, C., Frisén, J., Dragunow, M., Faull, R. L. M., & Eriksson, P. S. (2007). Human Neuroblasts Migrate to the Olfactory Bulb via a Lateral Ventricular Extension. *Science*, *315*(5816), 1243–1248. https://doi.org/10.1126/science.1136415

Davies, S. P., Reddy, H., Caivano, M., & Cohen, P. (2000). Specificity and mechanism of action of some commonly used protein kinase inhibitors. In *Biochem. J* (Vol. 351).

Deryugina, E. I., & Bourdon, M. A. (1996). Tenascin mediates human glioma cell migration and modulates cell migrationon fibronectin. *Journal of Cell Science*, *109*, 643–652.

Dhillon, A. S., Hagan, S., Rath, O., & Kolch, W. (2007). MAP kinase signalling pathways in cancer. In *Oncogene* (Vol. 26, Issue 22, pp. 3279–3290). https://doi.org/10.1038/sj.onc.1210421

Ditlevsen, D. K., Povlsen, G. K., Berezin, V., & Bock, E. (2008). NCAM-induced intracellular signaling revisited. In *Journal of Neuroscience Research* (Vol. 86, Issue 4, pp. 727–743). https://doi.org/10.1002/jnr.21551

Dontula, R., Dinasarapu, A., Chetty, C., Pannuru, P., Herbert, E., Ozer, H., & Lakka, S. S. (2013). MicroRNA 203 Modulates Glioma Cell Migration via Robo1/ERK/MMP-9 Signaling. *Genes and Cancer*, *4*(7–8), 285–296. https://doi.org/10.1177/1947601913500141

Dull, A. B., Wilsker, D., Hollingshead, M., Mazcko, C., Annunziata, C. M., Leblanc, A. K., Doroshow, J. H., Kinders, R. J., & Parchment, R. E. (2018). Development of a quantitative pharmacodynamic assay for apoptosis in fixed tumor tissue and its application in distinguishing cytotoxic drug−induced DNA double strand breaks from DNA double strand breaks associated with apoptosis. In *Oncotarget* (Vol. 9, Issue 24). www.oncotarget.com

Duncia, J. v, Iii, S., Anne Higley, C., Pitts, W. J., Wityak, J., Frietze, W. E., Wayne Rankin, F., Sun, J.-H., Earl, R. A., Christine Tabaka, A., Teleha, C. A., Blom, K. F., Favata, M. F., Manos, E. J., Daulerio, A. J., Stradley, D. A., Horiuchi, K., Copeland, R. A., Scherle, P. A., … Olson, R. E. (1998). MEK INHIBITORS: THE CHEMISTRY AND BIOLOGICAL ACTIVITY OF U0126, ITS ANALOGS, AND CYCLIZATION PRODUCTS. *Bioorganic & Medicinal Chemistry Letters*, *8*, 2839–2844.

Duval, K., Grover, H., Han, L. H., Mou, Y., Pegoraro, A. F., Fredberg, J., & Chen, Z. (2017). Modeling physiological events in 2D vs. 3D cell culture. In *Physiology* (Vol. 32, Issue 4, pp. 266–277). American Physiological Society. https://doi.org/10.1152/physiol.00036.2016

Ellis, F. (1969). Dose, Time and Fractionation: A Clinical Hypothesis. *Clinical Radiology*, *20*(1), 1–7.

English, J. M., & Cobb, M. H. (2002). Pharmacological inhibitors of MAPK pathways. *TRENDS in Pharmacological Sciences*, *23*(1). http://tips.trends.com0165-6147/02/$-seefrontmatter

Erasimus, H., Gobin, M., Niclou, S., & van Dyck, E. (2016). DNA repair mechanisms and their clinical impact in glioblastoma. In *Mutation Research - Reviews in Mutation Research* (Vol. 769, pp. 19–35). Elsevier B.V. https://doi.org/10.1016/j.mrrev.2016.05.005

Flaherty, K. T., Robert, C., Hersey, P., Nathan, P., Garbe, C., Milhem, M., Demidov, L. v., Hassel, J. C., Rutkowski, P., Mohr, P., Dummer, R., Trefzer, U., Larkin, J. M. G., Utikal, J., Dreno, B., Nyakas, M., Middleton, M. R., Becker, J. C., Casey, M., … Schadendorf, D. (2012). Improved Survival with MEK Inhibition in BRAF-Mutated Melanoma. *New England Journal of Medicine*, *367*(2), 107–114. https://doi.org/10.1056/nejmoa1203421

Friedl, P., & Gilmour, D. (2009). Collective cell migration in morphogenesis, regeneration and cancer. In *Nature Reviews Molecular Cell Biology* (Vol. 10, Issue 7, pp. 445–457). https://doi.org/10.1038/nrm2720

Friedl, P., & Wolf, K. (2003). Tumour-cell invasion and migration: Diversity and escape mechanisms. In *Nature Reviews Cancer* (Vol. 3, Issue 5, pp. 362–374). https://doi.org/10.1038/nrc1075

Fu, Liu, Halim, Ju, Luo, & Song. (2019). Mesenchymal Stem Cell Migration and Tissue Repair. *Cells*, *8*(8), 784. https://doi.org/10.3390/cells8080784

Fujimoto, I., Bruses, J. L., & Rutishauser, U. (2001). Regulation of cell adhesion by polysialic acid. Effects on cadherin, immunoglobulin cell adhesion molecule, and integrin function and independence from neural cell adhesion molecule binding or signaling activity. *Journal of Biological Chemistry*, *276*(34), 31745–31751. https://doi.org/10.1074/jbc.M104525200

Gao, D., Vahdat, L. T., Wong, S., Chang, J. C., & Mittal, V. (2012). Microenvironmental regulation of epithelial-mesenchymal transitionsin cancer. In *Cancer Research* (Vol. 72, Issue 19, pp. 4883–4889). https://doi.org/10.1158/0008-5472.CAN-12-1223

Gao, J., Wang, Y., Yang, J., Zhang, W., Meng, K., Sun, Y., Li, Y., & He, Q. Y. (2019). RNF128 promotes invasion and metastasis via the EGFR/MAPK/MMP-2 pathway in esophageal squamous cell carcinoma. *Cancers*, *11*(6). https://doi.org/10.3390/cancers11060840

Gensbittel, V., Kräter, M., Harlepp, S., Busnelli, I., Guck, J., & Goetz, J. G. (2021). Mechanical Adaptability of Tumor Cells in Metastasis. In *Developmental Cell* (Vol. 56, Issue 2, pp. 164–179). Cell Press. https://doi.org/10.1016/j.devcel.2020.10.011

Gerashchenko, T. S., Novikov, N. M., Krakhmal, N. v., Zolotaryova, S. Y., Zavyalova, M. v., Cherdyntseva, N. v., Denisov, E. v., & Perelmuter, V. M. (2019). Markers of Cancer Cell Invasion: Are They Good Enough? *Journal of Clinical Medicine*, *8*(8), 1092. https://doi.org/10.3390/jcm8081092

Gianfaldoni, S., Gianfaldoni, R., Wollina, U., Lotti, J., Tchernev, G., & Lotti, T. (2017). An overview on radiotherapy: From its history to its current applications in dermatology. *Open Access Macedonian Journal of Medical Sciences*, *5*(4 Special Issue GlobalDermatology), 521–525. https://doi.org/10.3889/oamjms.2017.122

Gong, P., Wang, Y., Liu, G., Zhang, J., & Wang, Z. (2013). New Insight into Ki67 Expression at the Invasive Front in Breast Cancer. *PLoS ONE*, *8*(1). https://doi.org/10.1371/journal.pone.0054912

Grigore, A. D., Jolly, M. K., Jia, D., Farach-Carson, M. C., & Levine, H. (2016). Tumor budding: The name is EMT. partial EMT. In *Journal of Clinical Medicine* (Vol. 5, Issue 5). MDPI. https://doi.org/10.3390/jcm5050051

Guan, F., Wang, X., & He, F. (2015). Promotion of cell migration by neural cell adhesion molecule (NCAM) is enhanced by PSA in a polysialyltransferase-specific manner. *PLoS ONE*, *10*(4). https://doi.org/10.1371/journal.pone.0124237

Gudbergsson, J. M., Kostrikov, S., Johnsen, K. B., Fliedner, F. P., Stolberg, C. B., Humle, N., Hansen, A. E., Kristensen, B. W., Christiansen, G., Kjær, A., Andresen, T. L., & Duroux, M. (2019). A tumorsphere model of glioblastoma multiforme with intratumoral heterogeneity for quantitative analysis of cellular migration and drug response. *Experimental Cell Research*, *379*(1), 73–82. https://doi.org/10.1016/j.yexcr.2019.03.031

Gundelach, J., & Koch, M. (2020). EndoN treatment allows neuroblasts to leave the rostral migratory stream and migrate towards a lesion within the prefrontal cortex of rats. *Neural Regeneration Research*, *15*(9), 1740–1747. https://doi.org/10.4103/1673-5374.276335

Guo, Y., Pan, W., Liu, S., Shen, Z., Xu, Y., & Hu, L. (2020). ERK/MAPK signalling pathway and tumorigenesis (Review). *Experimental and Therapeutic Medicine*. https://doi.org/10.3892/etm.2020.8454

Gupta, A., & Dwivedi, T. (2017). A simplified overview of World Health Organization classification update of central nervous system tumors 2016. In *Journal of Neurosciences in Rural Practice* (Vol. 8, Issue 4, pp. 629–641). Medknow Publications. https://doi.org/10.4103/jnrp.jnrp_168_17

Hanahan, D. (2022). Hallmarks of Cancer: New Dimensions. In *Cancer Discovery* (Vol. 12, Issue 1, pp. 31–46). American Association for Cancer Research Inc. https://doi.org/10.1158/2159-8290.CD-21-1059

Hanahan, D., & Weinberg, R. A. (2011a). Hallmarks of cancer: The next generation. In *Cell* (Vol. 144, Issue 5, pp. 646–674). https://doi.org/10.1016/j.cell.2011.02.013

Hanahan, D., & Weinberg, R. A. (2011b). Hallmarks of cancer: The next generation. In *Cell* (Vol. 144, Issue 5, pp. 646–674). https://doi.org/10.1016/j.cell.2011.02.013

Hegi, M. E., Diserens, A.-C., Gorlia, T., Hamou, M.-F., de Tribolet, N., Weller, M., Kros, J. M., Hainfellner, J. A., Mason, W., Mariani, L., Bromberg, E. C., Hau, P., Mirimanoff, R. O., Cairncross, J. G., Janzer, R. C., & Stupp, R. (2005). MGMT Gene Silencing and Benefit from Temozolomide in Glioblastoma. *The New England Journal of Medicine*, *352*(10), 997–1003. www.nejm.org

Hildebrandt, H., Becker, C., Glã¼er, S., Rã ¶sner, H., Gerardy-Schahn, R., & Rahmann, H. (1998). Polysialic Acid on the Neural Cell Adhesion Molecule Correlates with Expression of Polysialyltransferases and Promotes Neuroblastoma Cell Growth1. In *CANCER RESEARCH* (Vol. 58). http://aacrjournals.org/cancerres/article-pdf/58/4/779/2469220/cr0580040779.pdf

Hinkle, C. L., Diestel, S., Lieberman, J., & Maness, P. F. (2006). Metalloprotease-induced ectodomain shedding of neural cell adhesion molecule (NCAM). *Journal of Neurobiology*, *66*(12), 1378–1395. https://doi.org/10.1002/neu.20257

Hoffman, S., & Edelman, G. M. (1983). Kinetics of homophilic binding byembryonic and adult forms of neural cell adhesion molecule. *Proc.Natl.Acad*, *80*, 5762–5766.

Horstkorte, R., Schachner, M., Magyar, J. P., Vorherr, T., Schmitz, B., & Schmitz, B. (1993). The Fourth Immunoglobulin-like Domain of NCAM Contains a Carbohydrate Recognition Domain for Oligomannosidic Glycans Implicated in Association with L1 and Neurite Outgrowth. In *The Journal of Cell Biology* (Vol. 121, Issue 6).

Hu, H., & Tomasiewicz, H. (1996). The Role of Polysialic Acid in Migration of Olfactory Bulb Interneuron Precursors in the Subventricular Zone. In *Neuron* (Vol. 16).

Jackson, M., Hassiotou, F., & Nowak, A. (2014). Glioblastoma stem-like cells: At the root of tumor recurrence and a therapeutic target. In *Carcinogenesis* (Vol. 36, Issue 2, pp. 177–185). Oxford University Press. https://doi.org/10.1093/carcin/bgu243

Jackson, S. P., & Bartek, J. (2009). The DNA-damage response in human biology and disease. In *Nature* (Vol. 461, Issue 7267, pp. 1071–1078). https://doi.org/10.1038/nature08467

Johnson, C. P., Fujimoto, I., Rutishauser, U., & Leckband, D. E. (2005). Direct evidence that Neural Cell Adhesion Molecule (NCAM) polysialylation increases intermembrane repulsion and abrogates adhesion. *Journal of Biological Chemistry*, *280*(1), 137–145. https://doi.org/10.1074/jbc.M410216200

Kang, S. G., Cheong, J. H., Huh, Y. M., Kim, E. H., Kim, S. H., & Chang, J. H. (2015). Potential use of glioblastoma tumorsphere: Clinical credentialing. In *Archives of Pharmacal Research* (Vol. 38, Issue 3, pp. 402–407). Pharmaceutical Society of Korea. https://doi.org/10.1007/s12272-015-0564-0

Kim, Y. (2013). Regulation of cell proliferation and migration in glioblastoma: New therapeutic approach. *Frontiers in Oncology*, *3 MAR*. https://doi.org/10.3389/fonc.2013.00053

Kojima, N., Tachida, Y., Yoshida, Y., & Tsuji, S. (1996). *Characterization of Mouse ST8Sia II (STX) as a Neural Cell Adhesion Molecule-specific Polysialic Acid Synthase*.

Kolkova, K., Novitskaya, V., Pedersen, N., Berezin, V., & Bock, E. (1994). *Neural Cell Adhesion Molecule-Stimulated Neurite Outgrowth Depends on Activation of Protein Kinase C and the Ras-Mitogen-Activated Protein Kinase Pathway*.

Kramer, N., Walzl, A., Unger, C., Rosner, M., Krupitza, G., Hengstschläger, M., & Dolznig, H. (2013). In vitro cell migration and invasion assays. In *Mutation Research - Reviews in Mutation Research* (Vol. 752, Issue 1, pp. 10–24). https://doi.org/10.1016/j.mrrev.2012.08.001

Kurosaka, S., & Kashina, A. (2008). Cell biology of embryonic migration. In *Birth Defects Research Part C - Embryo Today: Reviews* (Vol. 84, Issue 2, pp. 102–122). https://doi.org/10.1002/bdrc.20125

Lakka, S. S., Jasti, S. L., Gondi, C., Boyd, D., Chandrasekar, N., Dinh, D. H., Olivero, W. C., Gujrati, M., & Rao, J. S. (2002). Downregulation of MMP-9 in ERK-mutated stable transfectants inhibits glioma invasion in vitro. *Oncogene*, *21*, 5601–5608. https://doi.org/10.1038/sj.onc

Lambert, A. W., Pattabiraman, D. R., & Weinberg, R. A. (2017). Emerging Biological Principles of Metastasis. In *Cell* (Vol. 168, Issue 4, pp. 670–691). Cell Press. https://doi.org/10.1016/j.cell.2016.11.037

Lamouille, S., Xu, J., & Derynck, R. (2014). Molecular mechanisms of epithelial-mesenchymal transition. In *Nature Reviews Molecular Cell Biology* (Vol. 15, Issue 3, pp. 178–196). https://doi.org/10.1038/nrm3758

Lan, X., Jörg, D. J., Cavalli, F. M. G., Richards, L. M., Nguyen, L. v., Vanner, R. J., Guilhamon, P., Lee, L., Kushida, M. M., Pellacani, D., Park, N. I., Coutinho, F. J., Whetstone, H., Selvadurai, H. J., Che, C., Luu, B., Carles, A., Moksa, M., Rastegar, N., … Dirks, P. B. (2017). Fate mapping of human glioblastoma reveals an invariant stem cell hierarchy. *Nature*, *549*(7671), 227–232. https://doi.org/10.1038/nature23666

Lee, J., Kotliarova, S., Kotliarov, Y., Li, A., Su, Q., Donin, N. M., Pastorino, S., Purow, B. W., Christopher, N., Zhang, W., Park, J. K., & Fine, H. A. (2006). Tumor stem cells derived from glioblastomas cultured in bFGF and EGF more closely mirror the phenotype and genotype of primary tumors than do serum-cultured cell lines. *Cancer Cell*, *9*(5), 391–403. https://doi.org/10.1016/j.ccr.2006.03.030

Lesniak, M. S., & Brem, H. (2004). Targeted therapy for brain tumours. In *Nature Reviews Drug Discovery* (Vol. 3, Issue 6, pp. 499–508). Nature Publishing Group. https://doi.org/10.1038/nrd1414

Liu, L., & Gerson2, S. (1996). Mismatch Repair Mutations Override Alkyltransferase in Conferring Resistance to Temozolomide but not to 1,3-Bis(2-chloroethyl)nitrosourea'. *Cancer Research*, *56*, 5375–5379. http://aacrjournals.org/cancerres/article-pdf/56/23/5375/2462072/cr0560235375.pdf

Liu, Q., Xu, X., Zhao, M., Wei, Z., Li, X., Zhang, X., Liu, Z., Gong, Y., & Shao, C. (2015). Berberine induces senescence of human glioblastoma cells by downregulating the EGFR-MEK-ERK signaling pathway. *Molecular Cancer Therapeutics*, *14*(2), 355–363. https://doi.org/10.1158/1535-7163.MCT-14-0634

Liu, Y., Beyer, A., & Aebersold, R. (2016). On the Dependency of Cellular Protein Levels on mRNA Abundance. In *Cell* (Vol. 165, Issue 3, pp. 535–550). Cell Press. https://doi.org/10.1016/j.cell.2016.03.014

Livak, K. J., & Schmittgen, T. D. (2001). Analysis of relative gene expression data using real-time quantitative PCR and the 2-ΔΔCT method. *Methods*, *25*(4), 402–408. https://doi.org/10.1006/meth.2001.1262

Louis, D. N., Ohgaki, H., Wiestler, O. D., Cavenee, W. K., Burger, P. C., Jouvet, A., Scheithauer, B. W., & Kleihues, P. (2007). The 2007 WHO classification of tumours of the central nervous system. In *Acta Neuropathologica* (Vol. 114, Issue 2, pp. 97–109). https://doi.org/10.1007/s00401-007-0243-4

Louis, D. N., Perry, A., Reifenberger, G., von Deimling, A., Figarella-Branger, D., Cavenee, W. K., Ohgaki, H., Wiestler, O. D., Kleihues, P., & Ellison, D. W. (2016). The 2016 World Health Organization Classification of Tumors of the Central Nervous System: a summary. *Acta Neuropathologica*, *131*(6), 803–820. https://doi.org/10.1007/s00401-016-1545-1

Louis, D. N., Perry, A., Wesseling, P., Brat, D. J., Cree, I. A., Figarella-Branger, D., Hawkins, C., Ng, H. K., Pfister, S. M., Reifenberger, G., Soffietti, R., von Deimling, A., & Ellison, D. W. (2021). The 2021 WHO classification of tumors of the central nervous system: A summary. *Neuro-Oncology*, *23*(8), 1231–1251. https://doi.org/10.1093/neuonc/noab106

McLendon, R., Friedman, A., Bigner, D., van Meir, E. G., Brat, D. J., Mastrogianakis, G. M., Olson, J. J., Mikkelsen, T., Lehman, N., Aldape, K., Yung, W. K. A., Bogler, O., Weinstein, J. N., VandenBerg, S., Berger, M., Prados, M., Muzny, D., Morgan, M., Scherer, S., … Thomson, E. (2008). Comprehensive genomic characterization defines human glioblastoma genes and core pathways. *Nature*, *455*(7216), 1061–1068. https://doi.org/10.1038/nature07385

Mione, J., Manrique, C., Duhoo, Y., Roman, F. S., & Guiraudie-Capraz, G. (2016). Expression of polysialyltransferases (STX and PST) in adult rat olfactory bulb after an olfactory associative discrimination task. *Neurobiology of Learning and Memory*, *130*, 52–60. https://doi.org/10.1016/j.nlm.2016.01.011

Mody, N., Leitch, J., Armstrong, C., Dixon, J., & Cohen, P. (2001). Effects of MAP kinase cascade inhibitors on the MKK5/ERK5 pathway. *Federation of European Biochemical Societies*, 21–24.

Muhlenhoff, M., Eckhardt, M., Bethe, A., Frosch, M., & Gerardy-Schahn1, R. (1996). Autocatalytic polysialylation of polysialyltransferase-1. In *The EMBO Journal* (Vol. 15, Issue 24).

Mulcahy, E. Q. X., Colón, R. R., & Abounader, R. (2020). Hgf/met signaling in malignant brain tumors. *International Journal of Molecular Sciences*, *21*(20), 1–18. https://doi.org/10.3390/ijms21207546

Muller, D., Wang, C., Skibo, G., Toni, N., & Cremer, H. (1996). PSA-NCAM Is Required for Activity-Induced Synaptic Plasticity. In *Neuron* (Vol. 17).

Murray, H. C., Low, V. F., Swanson, M. E. V., Dieriks, B. v., Turner, C., Faull, R. L. M., & Curtis, M. A. (2016). Distribution of PSA-NCAM in normal, Alzheimer's and Parkinson's disease human brain. *Neuroscience*, *330*, 359–375. https://doi.org/10.1016/j.neuroscience.2016.06.003

Ochs, K., & Kaina, B. (2000). Apoptosis Induced by DNA Damage O 6-Methylguanine Is Bcl-2 and Caspase-9/3 Regulated and Fas/Caspase-8 Independent 1. *Cancer Research*, *60*, 5815–5824.

Ohgaki, H., & Kleihues, P. (2013). The definition of primary and secondary glioblastoma. In *Clinical Cancer Research* (Vol. 19, Issue 4, pp. 764–772). https://doi.org/10.1158/1078-0432.CCR-12-3002

Orringer, D., Lau, D., Khatri, S., Zamora-Berridi, G. J., Zhang, K., Wu, C., Chaudhary, N., & Sagher, O. (2012). Extent of resection in patients with glioblastoma: Limiting factors, Perception of resectability, and effect on survival. *Journal of Neurosurgery*, *117*(5), 851–859. https://doi.org/10.3171/2012.8.JNS12234

Pandya, P., Orgaz, J. L., & Sanz-Moreno, V. (2017). Modes of invasion during tumour dissemination. In *Molecular oncology* (Vol. 11, Issue 1, pp. 5–27). https://doi.org/10.1002/1878-0261.12019

Paňková, K., Rösel, D., Novotný, M., & Brábek, J. (2010). The molecular mechanisms of transition between mesenchymal and amoeboid invasiveness in tumor cells. In *Cellular and Molecular Life Sciences* (Vol. 67, Issue 1, pp. 63–71). https://doi.org/10.1007/s00018-009-0132-1

Park, T. I. H., Smyth, L. C. D., Aalderink, M., Woolf, Z. R., Rustenhoven, J., Lee, K., Jansson, D., Smith, A., Feng, S., Correia, J., Heppner, P., Schweder, P., Mee, E., & Dragunow, M. (2022). Routine culture and study of adult human brain cells from neurosurgical specimens. In *Nature Protocols* (Vol. 17, Issue 2, pp. 190–221). Nature Research. https://doi.org/10.1038/s41596-021-00637-8

Perry, J. R., Laperriere, N., O'Callaghan, C. J., Brandes, A. A., Menten, J., Phillips, C., Fay, M., Nishikawa, R., Cairncross, J. G., Roa, W., Osoba, D., Rossiter, J. P., Sahgal, A., Hirte, H., Laigle-Donadey, F., Franceschi, E., Chinot, O., Golfinopoulos, V., Fariselli, L., … Mason, W. P. (2017).

Short-Course Radiation plus Temozolomide in Elderly Patients with Glioblastoma. *New England Journal of Medicine*, *376*(11), 1027–1037. https://doi.org/10.1056/nejmoa1611977

Petridis, A. K., el Maarouf, A., & Rutishauser, U. (2004). Polysialic acid regulates cell contact-dependent neuronal differentiation of progenitor cells from the subventricular zone. *Developmental Dynamics*, *230*(4), 675–684. https://doi.org/10.1002/dvdy.20094

Planagumà, J., Liljeström, M., Alameda, F., Bützow, R., Virtanen, I., Reventós, J., & Hukkanen, M. (2011). Matrix metalloproteinase-2 and matrix metalloproteinase-9 codistribute with transcription factors RUNX1/AML1 and ETV5/ERM at the invasive front of endometrial and ovarian carcinoma. *Human Pathology*, *42*(1), 57–67. https://doi.org/10.1016/j.humpath.2010.01.025

Pollard, S. M., Yoshikawa, K., Clarke, I. D., Danovi, D., Stricker, S., Russell, R., Bayani, J., Head, R., Lee, M., Bernstein, M., Squire, J. A., Smith, A., & Dirks, P. (2009). Glioma Stem Cell Lines Expanded in Adherent Culture Have Tumor-Specific Phenotypes and Are Suitable for Chemical and Genetic Screens. *Cell Stem Cell*, *4*(6), 568–580. https://doi.org/10.1016/j.stem.2009.03.014

Qian, X. C., & Brent, T. P. (1997). Methylation Hot Spots in the 5' Flanking Region Denote Silencing of the 06-Methylguanine-DNA Methyltransferase Gene'. *Cancer Reserach*, *57*, 3672–3677. http://aacrjournals.org/cancerres/article-pdf/57/17/3672/2464495/cr0570173672.pdf

Riahi, R., Yang, Y., Zhang, D. D., & Wong, P. K. (2012). Advances in wound-healing assays for probing collective cell migration. In *Journal of Laboratory Automation* (Vol. 17, Issue 1, pp. 59–65). SAGE Publications Inc. https://doi.org/10.1177/2211068211426550

Rowe, R. G., & Weiss, S. J. (2009). Navigating ECM barriers at the invasive front: The cancer cell-stroma interface. In *Annual Review of Cell and Developmental Biology* (Vol. 25, pp. 567–595). https://doi.org/10.1146/annurev.cellbio.24.110707.175315

Rutishauser, U. (2008). Polysialic acid in the plasticity of the developing and adult vertebrate nervous system. In *Nature Reviews Neuroscience* (Vol. 9, Issue 1, pp. 26–35). https://doi.org/10.1038/nrn2285

Sahai, E. (2005). Mechanisms of cancer cell invasion. In *Current Opinion in Genetics and Development* (Vol. 15, Issue 1, pp. 87–96). https://doi.org/10.1016/j.gde.2004.12.002

Sahara, N., & Takeshita, A. (2004). Prognostic significance of surface markers expressed in multiple myeloma: CD56 and other antigens. In *Leukemia and Lymphoma* (Vol. 45, Issue 1, pp. 61–65). https://doi.org/10.1080/1042819031000149377

Sanai, N., Alvarez-Buylla, A., & Berger, M. S. (2005). Neural Stem Cells and the Origin of Gliomas. In *n engl j med* (Vol. 8). www.nejm.org

Sasaki, H., Yoshida, K., Ikeda, E., Asou, H., Inaba, M., Otani, M., & Kawase, T. (1998). Expression of the Neural Cell Adhesion Molecule in Astrocytic Tumors An Inverse Correlation with Malignancy. *American Cancer Society*, *82*(10), 1921–1931.

Savagner, P. (2015). Epithelial-mesenchymal transitions: From cell plasticity to concept elasticity. In *Current Topics in Developmental Biology* (Vol. 112, pp. 273–300). Academic Press Inc. https://doi.org/10.1016/bs.ctdb.2014.11.021

Schindelin, J., Arganda-Carreras, I., Frise, E., Kaynig, V., Longair, M., Pietzsch, T., Preibisch, S., Rueden, C., Saalfeld, S., Schmid, B., Tinevez, J. Y., White, D. J., Hartenstein, V., Eliceiri, K., Tomancak, P., & Cardona, A. (2012). Fiji: An open-source platform for biological-image analysis. In *Nature Methods* (Vol. 9, Issue 7, pp. 676–682). https://doi.org/10.1038/nmeth.2019

Seidenfaden, R., Krauter, A., Schertzinger, F., Gerardy-Schahn, R., & Hildebrandt, H. (2003). Polysialic Acid Directs Tumor Cell Growth by Controlling Heterophilic Neural Cell Adhesion Molecule Interactions. *Molecular and Cellular Biology*, *23*(16), 5908–5918. https://doi.org/10.1128/mcb.23.16.5908-5918.2003

Seifert, A., Glanz, D., Glaubitz, N., Horstkorte, R., & Bork, K. (2012). Polysialylation of the neural cell adhesion molecule: Interfering with polysialylation and migration in neuroblastoma cells. In *Archives of Biochemistry and Biophysics* (Vol. 524, Issue 1, pp. 56–63). https://doi.org/10.1016/j.abb.2012.04.011

Seki, T., & Arai, Y. (1993). *Highly Polysialylated Neural Cell Adhesion Molecule (NCAM-H) Is Expressed by Newly Generated Granule Cells in the Dentate Gyrus of the Adult Rat*.

Shankar, A., Kumar, S., Iskander, A., Varma, N. R. S., Janic, B., deCarvalho, A., Mikkelsen, T., Frank, J. A., Ali, M. M., Knight, R. A., Brown, S., & Arbab, A. S. (2014). Subcurative radiation significantly increases cell proliferation, invasion, and migration of primary glioblastoma multiforme in vivo. *Chinese Journal of Cancer*, *33*(3), 148–158. https://doi.org/10.5732/cjc.013.10095

Sharma, M., Sah, P., Sharma, S., & Radhakrishnan, R. (2013). Molecular changes in invasive front of oral cancer. In *Journal of Oral and Maxillofacial Pathology* (Vol. 17, Issue 2, pp. 240–247). https://doi.org/10.4103/0973-029X.119740

Sheline, G. E. (1977). Radiation Therapy of Brain Tumours. *Cancer*, *39*, 873–881.

Silvestri, I., Testa, F., Zappasodi, R., Cairo, C. W., Zhang, Y., Lupo, B., Galli, R., di Nicola, M., Venerando, B., & Tringali, C. (2014). Sialidase NEU4 is involved in glioblastoma stem cell survival. *Cell Death and Disease*, *5*(8). https://doi.org/10.1038/cddis.2014.349

Simon, C., Hicks, M., Nemechek, A., Mehta, R., O'Malley Jr, B., Goepfert, H., Flaitz, C., & Boyd, D. (1999). PD 098059, an inhibitor of ERK1 activation, attenuatesthe in vivo invasiveness of head and neck squamouscell carcinoma. *British Journal of Cancer*, *80*(9), 1412–1419.

Singh, S. K., Clarke, I. D., Terasaki, M., Bonn, V. E., Hawkins, C., Squire, J., & Dirks, P. B. (2003). Identification of a Cancer Stem Cell in Human Brain Tumours. *CANCER RESEARCH*, *63*, 5821–5828.

Smith, C. L., Kilic, O., Schiapparelli, P., Guerrero-Cazares, H., Kim, D. H., Sedora-Roman, N. I., Gupta, S., O'Donnell, T., Chaichana, K. L., Rodriguez, F. J., Abbadi, S., Park, J. S., Quiñones-Hinojosa, A., & Levchenko, A. (2016). Migration Phenotype of Brain-Cancer Cells Predicts Patient Outcomes. *Cell Reports*, *15*(12), 2616–2624. https://doi.org/10.1016/j.celrep.2016.05.042

Steelman, L. S., Pohnert, S. C., Shelton, J. G., Franklin, R. A., Bertrand, F. E., & McCubrey, J. A. (2004). JAK/STAT, Raf/MEK/ERK, PI3K/Akt and BCR-ABL in cell cycle progression and leukemogenesis. In *Leukemia* (Vol. 18, Issue 2, pp. 189–218). Nature Publishing Group. https://doi.org/10.1038/sj.leu.2403241

Stupp, R., Mason, W. P., van den Bent, M. J., Weller, M., Fisher, B., Taphoorn, M. J. B., Belanger, K., Brandes, A. A., Marosi, C., Bogdahn, U., Curschmann, J., Janzer, R. C., Ludwin, S. K., Gorlia, T., Allgeier, A., Lacombe, D., Cairncross, J. G., Eisenhauer, E., & Mirimanoff, R. O. (2005). *Radiotherapy plus Concomitant and Adjuvant Temozolomide for Glioblastoma*. www.nejm.org

Sulman, E. P., Ismaila, N., Armstrong, T. S., Tsien, C., Batchelor, T. T., Cloughesy, T., Galanis, E., Gilbert, M., Gondi, V., Lovely, M., Mehta, M., Mumber, M. P., Sloan, A., & Chang, S. M. (2017). Radiation therapy for glioblastoma: American Society of Clinical Oncology clinical practice guideline endorsement of the American Society for Radiation Oncology guideline. In *Journal of Clinical Oncology* (Vol. 35, Issue 3, pp. 361–369). American Society of Clinical Oncology. https://doi.org/10.1200/JCO.2016.70.7562

Sun, X., & Kaufman, P. D. (2018). Ki-67: more than a proliferation marker. In *Chromosoma* (Vol. 127, Issue 2, pp. 175–186). Springer Science and Business Media Deutschland GmbH. https://doi.org/10.1007/s00412-018-0659-8

Sun, Y., Liu, W. Z., Liu, T., Feng, X., Yang, N., & Zhou, H. F. (2015). Signaling pathway of MAPK/ERK in cell proliferation, differentiation, migration, senescence and apoptosis. In *Journal of Receptors and Signal Transduction* (Vol. 35, Issue 6, pp. 600–604). Taylor and Francis Ltd. https://doi.org/10.3109/10799893.2015.1030412

Sunayama, J., Matsuda, K. I., Sato, A., Tachibana, K., Suzuki, K., Narita, Y., Shibui, S., Sakurada, K., Kayama, T., Tomiyama, A., & Kitanaka, C. (2010). Crosstalk between the PI3K/mTOR and MEK/ERK pathways involved in the maintenance of self-renewal and tumorigenicity of glioblastoma stem-like cells. *Stem Cells*, *28*(11), 1930–1939. https://doi.org/10.1002/stem.521

Sung, H., Ferlay, J., Siegel, R. L., Laversanne, M., Soerjomataram, I., Jemal, A., & Bray, F. (2021). Global Cancer Statistics 2020: GLOBOCAN Estimates of Incidence and Mortality Worldwide for 36 Cancers in 185 Countries. *CA: A Cancer Journal for Clinicians*, *71*(3), 209–249. https://doi.org/10.3322/caac.21660

Suresh, S. (2007). Biomechanics and biophysics of cancer cells. *Acta Biomaterialia*, *3*(4), 413–438. https://doi.org/10.1016/j.actbio.2007.04.002

Suzuki, M., Suzuki, M., Nakayama, J., Suzuki, A., Angata, K., Chen, S., Sakai, K., Hagihara, K., Yamaguchi, Y., & Fukuda, M. (2005). Polysialic acid facilitates tumor invasion by glioma cells. *Glycobiology*, *15*(9), 887–894. https://doi.org/10.1093/glycob/cwi071

Tanaka, F., & Kawano, Y. (2000). Expression of Polysialic Acid and STX, a Human Polysialyltransferase, Is Correlated with Tumor Progression in Non-Small Cell Lung Cancer1 Lung biology View project Lung transplantation View project. *Cancer Research*, *60*, 3072–3080. https://www.researchgate.net/publication/242133906

Tang, C., Wang, M., Wang, P., Wang, L., Wu, Q., & Guo, W. (2019). Neural Stem Cells Behave as a Functional Niche for the Maturation of Newborn Neurons through the Secretion of PTN. *Neuron*, *101*(1), 32-44.e6. https://doi.org/10.1016/j.neuron.2018.10.051

Taylor, O. G., Brzozowski, J. S., & Skelding, K. A. (2019). Glioblastoma multiforme: An overview of emerging therapeutic targets. *Frontiers in Oncology*, *9*(SEP). https://doi.org/10.3389/fonc.2019.00963

Thakkar, J. P., Dolecek, T. A., Horbinski, C., Ostrom, Q. T., Lightner, D. D., Barnholtz-Sloan, J. S., & Villano, J. L. (2014). Epidemiologic and molecular prognostic review of glioblastoma. In *Cancer Epidemiology Biomarkers and Prevention* (Vol. 23, Issue 10, pp. 1985–1996). American Association for Cancer Research Inc. https://doi.org/10.1158/1055-9965.EPI-14-0275

Theodosis, D. T., ROUGONt, G., & Poulain, D. A. (1991). Retention of embryonic features by an adult neuronal system capable of plasticity: Polysialylated neural cell adhesion molecule in the hypothalamo-neurohypophysial system (neurosecretory system/polysialylation/immunochemistry). In *Proc. NatI. Acad. Sci. USA* (Vol. 88).

Thota, R., Johnson, D. B., & Sosman, J. A. (2015). Trametinib in the treatment of melanoma. *Expert Opinion on Biological Therapy*, *15*(5), 735–747. https://doi.org/10.1517/14712598.2015.1026323

Tomasiewicz, H., One, K., Yee, D., Thompson, C., Coridis, C., Rutishauser, U., & Magnuson, T. (1993). Genetic Deletion of a Neural Cell Adhesion Molecule Variant (N-CAM-180) Produces Distinct Defects in the Central Nervous System. In *Neuron* (Vol. 11).

Urbanska, K., Sokolowska, J., Szmidt, M., & Sysa, P. (2014). Glioblastoma multiforme - An overview. In *Wspolczesna Onkologia* (Vol. 18, Issue 5, pp. 307–312). Termedia Publishing House Ltd. https://doi.org/10.5114/wo.2014.40559

Ve Chazal, G., Durbec, P., Jankovski, A., Ve Rougon, G., & Cremer, H. (2000). *Consequences of Neural Cell Adhesion Molecule Deficiency on Cell Migration in the Rostral Migratory Stream of the Mouse*.

Verhaak, R. G. W., Hoadley, K. A., Purdom, E., Wang, V., Qi, Y., Wilkerson, M. D., Miller, C. R., Ding, L., Golub, T., Mesirov, J. P., Alexe, G., Lawrence, M., O'Kelly, M., Tamayo, P., Weir, B. A., Gabriel, S., Winckler, W., Gupta, S., Jakkula, L., … Hayes, D. N. (2010). Integrated Genomic Analysis Identifies Clinically Relevant Subtypes of Glioblastoma Characterized by Abnormalities in PDGFRA, IDH1, EGFR, and NF1. *Cancer Cell*, *17*(1), 98–110. https://doi.org/10.1016/j.ccr.2009.12.020

Vong, C. K., Wang, A., Dragunow, M., Park, T. I. H., & Shim, V. (2022). Robust Quantification of Regional Patterns of Migration in Three-Dimensional Cell Culture Models. *Journal of Medical and Biological Engineering*, *42*(1), 38–48. https://doi.org/10.1007/s40846-022-00680-0

Wang, J. P., & Hielscher, A. (2017). Fibronectin: How its aberrant expression in tumors may improve therapeutic targeting. In *Journal of Cancer* (Vol. 8, Issue 4, pp. 674–682). Ivyspring International Publisher. https://doi.org/10.7150/jca.16901

Wang, L., Liang, B., Li, Y. I., Liu, X., Huang, J., & Li, Y. M. (2019). What is the advance of extent of resection in glioblastoma surgical treatment - A systematic review. In *Chinese Neurosurgical Journal* (Vol. 5, Issue 1). BioMed Central Ltd. https://doi.org/10.1186/s41016-018-0150-7

Wang, Q., Hu, B., Hu, X., Kim, H., Squatrito, M., Scarpace, L., deCarvalho, A. C., Lyu, S., Li, P., Li, Y., Barthel, F., Cho, H. J., Lin, Y. H., Satani, N., Martinez-Ledesma, E., Zheng, S., Chang, E., Sauvé, C. E. G., Olar, A., … Verhaak, R. G. W. (2017). Tumor Evolution of Glioma-Intrinsic Gene Expression Subtypes Associates with Immunological Changes in the Microenvironment. *Cancer Cell*, *32*(1), 42-56.e6. https://doi.org/10.1016/j.ccell.2017.06.003

Wang, X., Enomoto, A., Asai, N., Kato, T., & Takahashi, M. (2016). Collective invasion of cancer: Perspectives from pathology and development. In *Pathology International* (Vol. 66, Issue 4, pp. 183–192). Blackwell Publishing. https://doi.org/10.1111/pin.12391

Wang, X., & Tournier, C. (2006). Regulation of cellular functions by the ERK5 signalling pathway. In *Cellular Signalling* (Vol. 18, Issue 6, pp. 753–760). https://doi.org/10.1016/j.cellsig.2005.11.003

Wild-Bode, C., Weller, M., Rimner, A., Dichgans, J., & Wick, W. (2001). Sublethal Irradiation Promotes Migration and Invasiveness of Glioma Cells: Implications for Radiotherapy of Human Glioblastoma 1. In *CANCER RESEARCH* (Vol. 61).

Yamaguchi, H., & Condeelis, J. (2007). Regulation of the actin cytoskeleton in cancer cell migration and invasion. In *Biochimica et Biophysica Acta - Molecular Cell Research* (Vol. 1773, Issue 5, pp. 642–652). https://doi.org/10.1016/j.bbamcr.2006.07.001

Yan, S. S., James, M. L., Kerstens, P., de Lambert, M., Robinson, B. A., & Yi, M. (2019). High-grade Glioma – A decade of care in Christchurch. *Journal of Medical Imaging and Radiation Oncology*, *63*(5), 665–673. https://doi.org/10.1111/1754-9485.12944

Younis, M., Faming, W., Hongyan, Z., Mengmeng, T., Hang, S., & Liudi, Y. (2019). Iguratimod encapsulated PLGA-NPs improves therapeutic outcome in glioma, glioma stem-like cells and temozolomide resistant glioma cells. *Nanomedicine: Nanotechnology, Biology, and Medicine*, *22*. https://doi.org/10.1016/j.nano.2019.102101

Yue, P. Y. K., Leung, E. P. Y., Mak, N. K., & Wong, R. N. S. (2010). A Simplified Method for Quantifying Cell Migration/Wound Healing in 96-Well Plates. *Journal of Biomolecular Screening*, *15*(4), 427–433. https://doi.org/10.1177/1087057110361772

Zbinden, M., Duquet, A., Lorente-Trigos, A., Ngwabyt, S. N., Borges, I., & Ruiz I. Altaba, A. (2010). NANOG regulates glioma stem cells and is essential in vivo acting in a cross-functional network with GLI1 and p53. *EMBO Journal*, *29*(15), 2659–2674. https://doi.org/10.1038/emboj.2010.137

Zepecki, J. P., Snyder, K. M., Moreno, M. M., Fajardo, E., Fiser, A., Ness, J., Sarkar, A., Toms, S. A., & Tapinos, N. (2019). Regulation of human glioma cell migration, tumor growth, and stemness gene expression using a Lck targeted inhibitor. *Oncogene*, *38*(10), 1734–1750. https://doi.org/10.1038/s41388-018-0546-z

Zhang, J., Stevens, M. F. G., & Bradshaw, T. D. (2012). Temozolomide: Mechanisms of Action, Repair and Resistance. In *Current Molecular Pharmacology* (Vol. 5).

Zhou, W., Ke, S. Q., Huang, Z., Flavahan, W., Fang, X., Paul, J., Wu, L., Sloan, A. E., McLendon, R. E., Li, X., Rich, J. N., & Bao, S. (2015). Periostin secreted by glioblastoma stem cells recruits M2 tumour-associated macrophages and promotes malignant growth. *Nature Cell Biology*, *17*(2), 170–182. https://doi.org/10.1038/ncb3090

Zlobec, I., & Lugli, A. (2009). Invasive front of colorectal cancer: Dynamic interface of pro-/anti-tumor factors. In *World Journal of Gastroenterology* (Vol. 15, Issue 47, pp. 5898–5906). Baishideng Publishing Group Co. https://doi.org/10.3748/wjg.15.5898